

Evaluating solvent efficiency for carbon capture: Comparative analysis of temperature, concentration and diffusivity effects

Maimoona Sharif^{a,*}, Tao Wang^{a,*}, Yanjie Xu^b, Mengxiang Fang^a, Haiqian Wu^b, Xiang Gao^a

^a State Key Laboratory of Clean Energy Utilization, Zhejiang University, Hangzhou, 310027, PR China

^b Xizi Clean Energy Equipment Manufacturing Co. Ltd., Hangzhou, 310021, PR China

ARTICLE INFO

Keywords:

CO₂ capture
Alkanolamines
Solvent concentration
Molecular dynamic simulation

ABSTRACT

In the pursuit of efficient carbon capture technologies, the selection and design of solvents play a pivotal role, directly impacting various crucial factors such as CO₂ absorption capacity, equipment size, and regeneration energy requirements. The primary focus is on optimizing solvent systems through a comprehensive analysis of intermolecular interaction intensity, diffusion coefficient, and intra-molecular interaction intensity. This study employs a molecular dynamics simulation model to identify the most suitable solvent system by assessing the effect of operating variables like temperature, concentration, interaction intensity, and diffusivity of various single and blended amine systems. The assessment utilizes the radial distribution function and mean square displacement analysis. The results indicate that intermolecular interactions with CO₂ are most significant in 30 wt% 2EAE, 40 wt% 2DMAE and 10% DMCA with 20% MCA ratio concentrations. TMPAD, in particular, stands out for its high repulsive interaction and low energy requirement for breaking the carbamate/bicarbonate ion. Diffusion behavior in various observed solvent systems is as follows: EAE > MEA > DMAE > MAE-DEAB > MAE-DMA2P > EAE-TMPAD > AMP-PZ > EAE-DEAB > MAE-TMPAD > EAE-DMA2P > MAE-DMAE > EAE-DMAE > TMPAD > MEA-AMP > DMA2P > DMCA-MCA > DEAB > MEA-PZ. Moreover, elevated temperatures facilitate enhanced diffusivity, leading to accelerated mass transfer rates. This implies the possibility of reducing the size of absorber units and lowering energy consumption. Further studies on heat of absorption and kinetic characteristics of solvent blends are necessary to ensure their practical applicability in carbon capture and industrial operations.

1. Introduction

The swift advancement of modern industrialization is closely linked to the burning of fossil fuels like coal, petroleum, and natural gas, fulfilling the increasing worldwide need for energy (Zhang et al., 2021). Nevertheless, this reliance carries a notable environmental toll, given that these procedures collectively account for roughly 83% of human-induced greenhouse gas discharges (EV, 2011). The advancement and utilization of Carbon Capture and Storage (CCS) technology represent a significant stride toward a low-carbon future and a more sustainable global ecosystem (Papadopoulos et al., 2017). Within the realm of diverse CCS techniques, chemical absorption stands out as a well-developed approach for CO₂ capture. However, even though it is a mature technology, the CO₂ absorption process still grapples with numerous hurdles. Chief among these issues is the substantial cost associated with the process, primarily driven by the energy-intensive

regeneration and the expenses tied to the selection and design of solvents. Beyond economic hurdles, environmental considerations come into play, as some solvents have adverse environmental impacts, raising concerns about toxicity and long-term sustainability (Melnikov et al., 2019). Therefore, researchers are actively addressing these multifaceted challenges through innovative solutions to enhance chemical absorption's overall efficiency, sustainability, and feasibility for CO₂ capture.

The selection of an efficient solvent system for CO₂ capture is critical to developing long-term and successful carbon capture methods. The implications of this decision extend throughout the capture process, affecting performance, energy consumption, and economic feasibility. A well-selected solvent system should strike a delicate balance between high selectivity for CO₂, which ensures maximum capture efficiency, and efficient desorption characteristics during the regeneration phase. The speed with which the solvent absorbs and releases CO₂ is crucial for obtaining realistic and scalable capture rates. As the global community

* Corresponding authors. State Key Laboratory of Clean Energy, Zhejiang University, Hangzhou, Zhejiang, PR China.

E-mail addresses: mona.chem@zju.edu.cn (M. Sharif), ogatnaw@zju.edu.cn (T. Wang).

<https://doi.org/10.1016/j.geoen.2024.212833>

Received 7 December 2023; Received in revised form 14 March 2024; Accepted 10 April 2024

Available online 18 April 2024

2949-8910/© 2024 Elsevier B.V. All rights reserved.

steps up efforts to combat climate change, the significance of discovering and implementing efficient solvent systems grows increasingly deeper. Hence, the present research is primarily dedicated to identifying an efficient solvent system through the analysis of both intermolecular and intramolecular interaction intensities, as well as the diffusion coefficient. Higher intermolecular interaction intensities facilitate CO₂ absorption, while intramolecular interaction intensity significantly influences CO₂ desorption during the regeneration phase. The diffusion coefficient is also a critical factor in ensuring a rapid CO₂ uptake rate. There is a noticeable gap in the existing research regarding diffusion coefficients and the nature of these interaction intensities, whether between molecules or within them, especially in various amine blends. This highlights the novelty and importance of our study as it aims to fill this gap in the literature. Furthermore, this study is an extension of our previous work and also provides a comprehensive comparison of various selected amine systems (Sharif et al., 2020, 2022, 2023a, 2023b).

Blended amine solvents have emerged as promising substitutions to MEA, leveraging the rapid absorption kinetics of primary or secondary amines and the advantageous low regeneration penalty of tertiary amines (Wang et al., 2021). In a comprehensive study by Muchan et al., (2017), hindered, primary, secondary, and tertiary amine (AMP, MEA, 2EAE, 2DMAE) solvent systems were systematically screened for CO₂ capture applications, considering the position of hydroxyl groups. The results highlighted that primary, secondary, and tertiary amines featuring one hydroxyl group attached to the amine structure (AMP, 2EAE, and 2DMAE) demonstrated superior CO₂ capture performance, positioning them as preferred choices for blended aqueous amine solutions (Muchan et al., 2017).

Zhang et al., 2007 conducted an examination of the CO₂ absorption characteristics of the DMCA-DPA (di-propylamine) system. Their focus was on highlighting DMCA as the primary absorbent due to its noteworthy capacity for CO₂ absorption and its ability to achieve low residual CO₂ loading after the regeneration process. Notably, DMCA displayed superior thermal stability compared to MEA (Zhang, 2007; Zhang et al., 2013). Furthermore, Zhang, 2014 highlighted MCA (N-methylcyclohexanone) as an exceptional promoter, showcasing its ability to significantly enhance CO₂ absorption rates and capacities compared to MEA (Zhang, 2014). MCA exhibited enhanced absorption, greater capacity for recycling, and reduced enthalpy of reaction in the context of CO₂ removal, compared to 30 lipophilic amines (Tan, 2010). Consequently, a blend of DMCA and MCA holds the potential to synergize the advantages of both components, leading to accelerated absorption rates, increased absorption capacity, and reduced desorption energy costs. Evaluating the performance of CO₂ absorption includes factors such as overall mass transfer coefficient, equilibrium solubility, rate of absorption and heat of absorption (Kadiwala et al., 2012). A study conducted by Kadiwala in 2012 reveals that 1DMA2P exhibits low heat of absorption and higher solubility compared to MDEA and MEA. Furthermore, 1DMA2P absorbs faster and has a higher capacity than MDEA, although at a slower mass transfer rate than MEA (Kadiwala et al., 2012). Given its superior performance, 1DMA2P emerges as a promising alternative solvent for CO₂ capture (Kadiwala et al., 2012).

Similarly, recent investigations have proposed several alternative solvents for CO₂ capture systems. Examples of these amines include N, N, N', N'-tetramethylpropane-1,3-diamine (TMPAD), 1-dimethylamino-2-propanol (1DMA2P), N-dimethylcyclohexanamine (DMCA), 4-diethylamino-2-butanol (DEAB), N, N-methylcyclohexanamine (MCA) and 2-methylamino ethanol (2MAE). The solvent selection criteria included low energy requirements for regeneration, higher CO₂ loading, low viscosity, and faster absorption rates. DEAB, identified as a tertiary amine, displays greater absorption capacity and low viscosity at 25 °C compared to MEA, making it an advantageous candidate for CO₂ capture (George et al., 2020). Reduced viscosity of DEAB results in lower operational expenses for the pump and circulation system, positioning DEAB as a cost-effective choice for liquid circulation in CO₂ capture systems (Naami et al., 2012). Tertiary amines, known for their CO₂

absorption capability and lower regeneration heat, prove highly effective for CO₂ removal, i.e., 1DMA2P has a higher CO₂ loading than MEA and MDEA, with a lower heat of absorption than MDEA (El Hadri et al., 2017). TMDAP, another tertiary amine, has higher CO₂ loading than 2DMAE due to the inclusion of an additional amino group that provides an extra site for CO₂ absorption. Because of its quick carbamate synthesis, piperazine is a preferred activator for alkanolamines in CO₂ capture systems and is used in blending with 2EAE and 2DMAE (Ahmad et al., 2018). Furthermore, the rate constant of PZ is ten times greater than that of standard MEA (Sodiq et al., 2018). These findings emphasize the potential of unconventional amines for use in CO₂ capture. This is the reason that the present study selected these solvents (as given in Table 1) to further explore the competences of the chosen amines in the realm of CO₂ capture.

The present study explores the potential of synergizing secondary and tertiary amines to mitigate the limitations associated with individual amines. Tertiary amines demonstrate absorption capacity and reduced heat of absorption when contrasted with traditional amines, even though with moderate reactivity (Ahmad et al., 2018). The molecular structure significantly influences the chemistry and kinetics of the amine-CO₂ reaction. Investigating the reaction mechanism reveals key steps and the role of specific chemical groups or interactions, guiding the understanding of desorption behavior. This knowledge aids in the development and optimization of CO₂ capture processes, aiming to enhance efficiency and reduce associated costs. Therefore, subsequent discussion delves into the reaction mechanisms of various amine types.

Numerous studies have explored the reactions of primary, secondary, tertiary, and hindered amines (Ahmad et al., 2018; Sodiq et al., 2018). It is evident that each amine type exhibits distinct reaction rates with CO₂.

Table 1
Diverse categories of amines investigated in the current study.

Name of Solvent	Structure	CAS No.
2-(ethylamino) ethanol (2EAE)		110-73-6
2 (methylamino) ethanol (2MAE)		109-83-1
2-(dimethylamino) ethanol (2DMAE)		108-01-0
4-Diethylamino-2-butanol (DEAB)		5867-64-1
1-Diethylamino-2-propanol (1DMA2P)		108-16-7
N,N,N',N'-Tetramethyl-1,3-propane diamine (TMPAD)		110-95-2
Piperazine (PZ)		110-85-0
2-amino-1-methyl-2propanol (AMP)		2854-16-2
N-methylcyclohexylamine (MCA)		100-60-7
N, N-dimethylcyclohexylamine (DMCA)		98-94-2

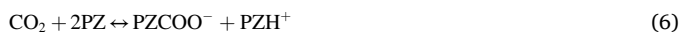
Typically, secondary and primary amines react more swiftly with CO₂, resulting in carbamate formation through proton transfer and zwitterion generation (Gao et al., 2019). Both primary and secondary amines demonstrate rapid CO₂ absorption, yielding zwitterions as depicted in Equation (1), followed by proton transfer to form carbamate, as illustrated in Equation (2).



The unique characteristics of tertiary amines, such as 2DMAE, are underscored, particularly in terms of their CO₂ loading capacity and reactivity Equation (4) and Equation (5). While tertiary amines offer higher potential CO₂ loading, their diminished reactivity highlights a trade-off that distinguishes them from primary and secondary amines. This discussion contributes to a nuanced understanding of the distinctive behavior of tertiary amines in CO₂ capture processes, shedding light on the complexities associated with their interaction with CO₂ and the resulting chemical transformations. Tertiary amines, including 2DMAE, follow a distinctive pathway for CO₂ absorption, resulting in the formation of bicarbonate. This is in contrast to primary and secondary amines, which typically undergo zwitterion formation during CO₂ absorption. The existing literature supports the notion that tertiary amines exhibit heightened loading capabilities at the expense of diminished reactivity (Donaldson et al., 1980). Equation (5) outlines the reaction mechanism responsible for bicarbonate generation in tertiary amines.



Piperazine, identified as a cyclic secondary diamine, has the ability to undergo a reaction with carbon dioxide, leading to the formation of a carbamate ion, a zwitterion, and a protonated carbamate. The detailed reaction mechanism for this process is depicted in Equations (6)–(8), as outlined in the relevant literature.



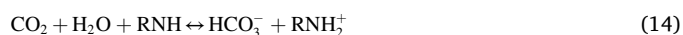
In the study by Sartori and Savage (1983), the sterically hindered amines due to the increased hindrance surrounding the amino group, results in unfavorable and slower carbamate formation Sartori and Savage (1983). However, for moderately hindered amines, the zwitterion to bicarbonate and protonated amine pathway may still contribute to the overall reaction rate (Sharif et al., 2020). The reactions below Equation (9)–Equation (10) illustrate that the primary occurrence in the reaction is through bicarbonate generation.



Most primary and secondary amines are known for their ability to absorb CO₂ via the zwitterion production pathway. However, MCA, a secondary amine, displayed an absorption capacity similar to that of the tertiary amine DMCA, reaching about 1 mol CO₂/mol amine (Wang et al., 2021). The overall reactions encompass zwitterion generation (Equation (11)) and proton transfer (Equation (12)), contributing to the enhanced CO₂ absorption capacity of DMCA-MCA system (Equation (13)). Specifically, the proton transfer process involving the MCA zwitterion and DMCA base heightens the CO₂ absorption capability of DMCA (Equation (16) (Wang et al., 2021)). Moreover, both ¹³CNMR and theoretical investigations have corroborated that the MCA carbamate is

unstable and readily transforms into bicarbonate, with bicarbonate emerging as the predominant product (Wang et al., 2021).

The combination of secondary and tertiary amines in the current work addresses a crucial aspect of solvent optimization for CO₂ capture. Tertiary amines, known for their absorption capacity and inferior absorption heat, bring valuable traits to the blend, even though their reactivity is moderate. Meanwhile, secondary amines contribute high reactivity, creating a synergistic effect in the blended solvent.



The study focuses on understanding the dynamics of this combination, particularly in terms of solvent concentration effect, carbamate stability and CO₂ diffusion rate by Molecular Dynamic Simulation. This study will provide a comparative analysis of various types of amines. Molecular dynamic simulations serve as an influential technique to explore the intricacies of these interactions (Meunier, 2005). This modeling technique offers a unique advantage in examining atomic-scale responses of structures. Molecular dynamics (MD) simulations faithfully replicate molecular structures from real-world macroscopic systems, making it a valuable tool for calculations that are challenging to reproduce in a laboratory setting (Meunier, 2005; Zhang et al., 2023). This methodology has demonstrated its reliability by aligning with existing experimental data, making it a versatile tool for assessing solvent behavior in various systems. MD simulations accelerate calculations and provide a visual representation of absorption reactions, offering an eco-friendly and cost-effective approach (Gao et al., 2023). The insights gained from this research have significant implications for improving the effectiveness of CO₂ capture developments and contribute towards the ongoing efforts in developing advanced solvent systems for sustainable carbon capture technologies.

2. Frame work of the study

In engineering studies, the application of computational techniques is essential for unraveling the underlying chemical processes involved in CO₂ absorption and for the development of novel absorbent compounds (Liang et al., 2016; Zhao et al., 2023; Wang et al., 2024). Molecular dynamic simulation, a method that resolves the fundamental equations governing particle motion, is employed in the current study to simulate CO₂ capture processes (Biovia and Material Studio, 2020). The simulations are conducted using a computer program within Material Studio, with structural data sourced from the Royal Society of Chemistry's database (ChemSpider, 2020). The simulation methodology encompasses several key stages like structure replication, energy minimization, amorphous box construction, model relaxation and intermolecular interaction and diffusivity analysis as presented in Fig. 1.

The selected structures are initially replicated and the energies of the replicated structures are minimized. An amorphous box is constructed to house the simulation. In the third step, the construction of the simulation box, or amorphous cell, is performed within the Material Studio's amorphous cell module. The size of the box is adjusted based on the number of inserted molecules. After construction, the molecules within the box may not be in their proper configurations, necessitating energy minimization to refine the structures. In industrial applications, equipment often takes cylindrical shapes for practical reasons, whereas simulations frequently employ cubic boxes for simplicity. The choice of box

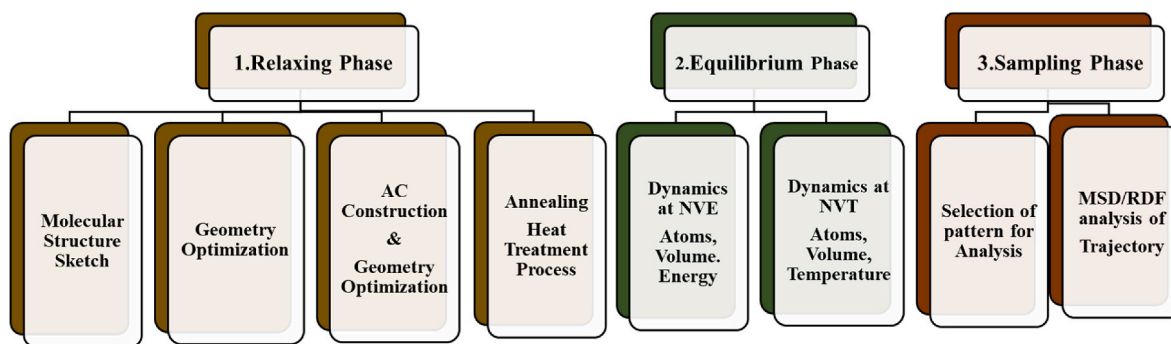


Fig. 1. Steps of model development in material studio.

shape can introduce boundary effects that impact the system's behavior. Molecules near the edges and corners of a cubic box may experience different forces compared to those in the bulk region, potentially leading to artifacts in simulation results. To address this, periodic boundary conditions are used in the radial direction, effectively creating an infinite cylindrical system. This minimizes boundary effects and ensures that the simulation results better represent the behavior within a cylindrical space (Leach, 2001). Validation of simulation results against experimental data or theoretical models specifically designed for cylindrical geometries is crucial for assessing their suitability and validity. This approach enhances the reliability and relevance of simulation outcomes and minimizes the influence of box shape on the simulated behavior. Periodic boundary conditions are pivotal in providing a framework for the study of infinite systems, reducing boundary effects, and facilitating comparisons with real-world systems. Consequently, they enhance the reliability and relevance of simulation outcomes.

The simulation model undergoes relaxation by simultaneously reducing pressure and energy. Equilibrium and Production Phases are conducted under NVE (constant number of particles, volume, and energy) and NVT (constant number of particles, volume, and temperature) conditions. Mean square and radial distribution functions are utilized for calculating intermolecular interactions and diffusivity across the chosen solvents (Sharif et al., 2020). Ensuring precise and reliable results in Material Studio simulations involves careful consideration of boundary conditions, forcefield selection, and step duration (Sharif et al., 2022). This study adopts a 1 fs step length and employs the COMPASS force field, recognized for its comprehensive evaluation of various compounds under diverse temperature and pressure conditions in the literature (Charati et al., 1998). The simulation begins with a 200-ps equilibration phase under NVE conditions to stabilize the system configuration and conserve energy. The subsequent transition to dynamic mode occurs under NVT conditions, employing the COMPASS force field and Ewald summation method to assess force field and interactions. Trajectory analysis, utilizing the forcite module in Material Studio, is performed on the final trajectories, and the input data for constructing the amorphous cell are summarized in supplementary materials (Tables S1, S2, and S3).

The radial distribution function (RDF) serves as a structural signifier applicable to compounds. This function acts as a metric gauging the likelihood of discovering neighboring molecules at a given distance 'r' from a reference molecule. By offering insights into the spatial organization of particles within a system, RDF stands as a pivotal tool in the exploration of molecular interactions and thermodynamic characteristics (Anslyn et al., 2006). Equation (17) succinctly formulates the radial distribution function as a thermodynamic entity, wherein the internal energy 'E' comprises the cumulative potential and kinetic energies denoted by 'U' (Hill, 1986).

$$E = \frac{3}{2} NkT + U \quad (17)$$

The potential energy, denoted as U, is derived through the integration of Equation (17). This equation can be reformulated as Equation

(18).

$$\frac{E}{NkT} = \frac{3}{2} + \frac{\rho}{2kT} \int u(r)g(r, \rho, T)4\pi r^2 dr \quad (18)$$

Furthermore, Equation (19) serves as a means to characterize the radial distribution function.

$$g(r) = \frac{1 < N(r, r + dr) >}{\rho 4\pi r^2 dr} \quad (19)$$

In the given context, 'ρ' denotes atom density, 'N' corresponds to the overall number of atoms and 'r' represents the spherical radius. The significance of the radial distribution function lies in three key aspects. Firstly, it proves valuable for pairwise additive potentials; having data of the RDF alone is enough to compute thermodynamic properties, with a particular focus on energy and pressure. Secondly, the radial distribution function serves as a well-established integral equation theory, enabling the approximation of the radial distribution function for a specific model under consideration. Thirdly, experimental determination of the radial distribution function can be conducted using neutron scattering techniques. This provides valuable insights into the spatial arrangement of particles in a system, aiding in the study of molecular interactions and thermodynamic properties (Zeebe, 2011; Chen et al., 2020).

Another important aspect analysed in the present study is mean square displacement analysis (MSD). The molecular diffusion coefficient D is computed in MD simulations through mean square displacement analysis, a process characterized by the Einstein relation. Equation (20) is employed for this purpose in MD simulations (Masy et al., 2013).

$$D_{(i, self)} = \frac{1}{6N_i} \lim_{\delta t \rightarrow 0} \frac{1}{m \cdot \delta t} \sum_{l=1}^{N_i} [(r_{(l,i)}((t + m \cdot \delta t)) - r_{(l,i)}(t))^2] \quad (20)$$

The equation incorporates essential features, including the number of molecules of components i denoted by 'Ni,' the simulation time step denoted by 'δt,' the total number of time steps represented by 'm,' and the position of the lth molecule of component i at time t given by r (l, i) (t). Utilizing these features, Equation (21) and Equation (22) enables the determination of the molecular diffusion coefficient D through MSD analysis, employing the Einstein relation (Masy et al., 2013).

$$6Dt = r\langle |r(t) - (0)|^2 \rangle = MSD(t) \quad (21)$$

$$D = \frac{1}{6} \frac{d}{dt} MSD(t) = \text{Constan } t \quad (22)$$

Equations (21) and (22) are employed for the computation of the diffusion coefficient, relying on the mean square displacement dimensions, where $r(t) = [x(t), y(t), z(t)]$ represents the directions of particles at t (time) (Zeebe, 2011). The slope of the MSD graph provides understandings about the rate at which particles diffuse, and the diffusion coefficient serves as a measure of how easily the molecules move through the system. Further details for Equation (17)-Equation (22) are

provided in supplementary materials in section 1.

3. Results & discussion

The present study involves the comprehensive screening of various solvents, analyzing solvent concentration, temperature effect on diffusion rate and both intermolecular (attractive) and intra-molecular (repulsive) in different solvent blends and pure solvents. The selected amines include 2EAE, 2DMAE, 2MAE, 2EAE-PZ, 2DMAE-PZ, PZ, AMP, DEAB, 1DMA2P, TMPAD, DMCA, and MCA. The findings of the study are presented one by one. Below are Fig. 2 and Fig. 3 illustrating the attributes of solvents and research paradigm of the study.

3.1. Investigation of interaction intensity in numerous types of amines

Table 2 represents a summary of the radial distribution function analysis, focusing on attractive and repulsive interactions between TMPAD, DEAB, MCA, DMCA, 2DMAE, PZ, AMP, 2MAE, 2EAE, and MEA with carbamate ions/bicarbonate ions and water. The study identifies specific interactions, such as $C_{\text{carbamate-O}_{\text{water}}}$ and $N_{\text{carbamate-H}_{\text{H}_2\text{O}}}$. Results indicate that $C_{\text{carbamate-O}_{\text{water}}}$ exhibits higher peak attractive interactions in certain solvents compared to $N_{\text{carbamate-H}_{\text{H}_2\text{O}}}$. For instance, MEA has the highest interaction at 3.75 Å, with a potential of 13.21% to locate atoms for interaction. Secondary amine 2MAE exhibits elevated interaction for $N_{\text{carbamate-H}_{\text{H}_2\text{O}}}$ compared to MEA. Piperazine, a secondary cyclic diamine, displays complex interactions with lower intensities in $C_{\text{carbamate-O}_{\text{water}}}$ and $N_{\text{carbamate-H}_{\text{H}_2\text{O}}}$ compared to other amines. Tertiary amine 1DMA2P demonstrates higher intensity for both interactions, highlighting unique attributes in studied solvent systems, while other tertiary amines like DMCA, DEAB, 2DMAE and TMPAD show varying interaction intensity. The detailed analysis reveals unique interaction patterns within tertiary amines, demonstrating specific behaviors of each amine. The interaction termed $C_{\text{Carbamate-O}_{\text{H}_2\text{O}}}$ is recognized as ion-dipole bonding. The heightened attractive interactions observed for $C_{\text{Carbamate-O}_{\text{H}_2\text{O}}}$ in amines can be attributed to the collaboration of carbamate ions with H_2O , generating bicarbonate and recycled amine. On the other hand, the interaction involving $N_{\text{Carbamate}}$ and $\text{H}_{\text{H}_2\text{O}}$ ($N_{\text{Carbamate-H}_{\text{H}_2\text{O}}}$) solely entails hydrogen bonding.

In this particular context, ion-dipole bonding ($C_{\text{Carbamate-O}_{\text{H}_2\text{O}}}$) exhibits greater potency compared to hydrogen bonding ($N_{\text{Carbamate}}$

$\text{H}_{\text{H}_2\text{O}}$), evident from the observed peaks occurring at shorter distances in $C_{\text{Carbamate-O}_{\text{H}_2\text{O}}}$. This observation aligns with established findings indicating that ion-dipole bonding tends to be more robust than hydrogen bonding (Hunt et al., 2015). Ion-dipole interactions occur between a fully charged ion and a partially charged dipole in a molecule. These interactions are prevalent in solutions where ions are present along with polar molecules. In the context of solvent systems, ion-dipole bonding is particularly relevant when considering the interactions between charged species, such as ions, and polar molecules like water. In the radial distribution function (RDF) analysis, the study highlights the presence of ion-dipole interactions between carbamate ions and water molecules. The charge centers of water molecules do not align uniformly, creating a dipole moment. This dipole induces the formation of ion-dipole interactions with the carbamate ions, showcasing the significance of charge distribution in facilitating these bonds (Hunt et al., 2015; Masiren et al., 2017). In the context of the study, the RDF analysis of attractive interactions reveals that monoethanolamine (MEA) exhibits the strongest attractive interaction. MEA is known to participate in hydrogen bonding due to the presence of hydrogen atoms bonded to oxygen in its structure. Additionally, both the tertiary amine 1DMA2P and the secondary amine 2EAE demonstrate elevated attractive interactions, suggesting the involvement of hydrogen bonding in these cases.

The high energy required for the stripping process, which tries to extract CO_2 from the carbamate ion during the amine absorption phase, is a big problem. Furthermore, the absorption potential must be spread out throughout numerous absorption cycles. The amine and CO_2 acid gas mixture separates during the stripping process in the regeneration column (Miccio et al., 2015; Harun et al., 2017a). The goal of this research is to look into the stabilization of carbamate ions throughout the process of extracting CO_2 from amine solutions. This research is critical in determining which amine requires the least amount of energy to break the bond. Table 2 summarizes the result of the repulsive interaction in the carbamate ion at 313 K. Breaking carbamate ions demands a significant amount of energy, resulting in the prominent observation of the repulsive interaction between $N_{\text{carbamate}}$ and $C_{\text{carbamate}}$. This repulsive interaction has a distinct peak that differs from the attractive interaction (Fig. 4). Unlike the attractive interaction, the repulsive interaction in this study had a single peak at a distance of 1.5 Å, indicating a quick and isolated occurrence. Table 2 contains a variety

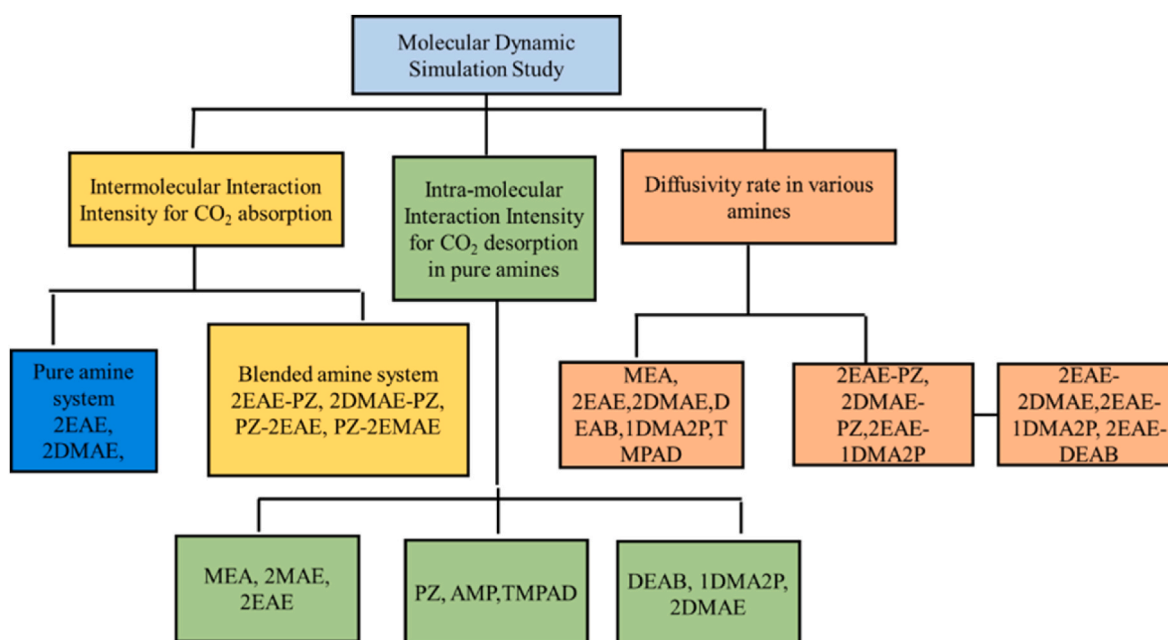


Fig. 2. Molecular Dynamic Study of Various selected Solvents in the Present Study.

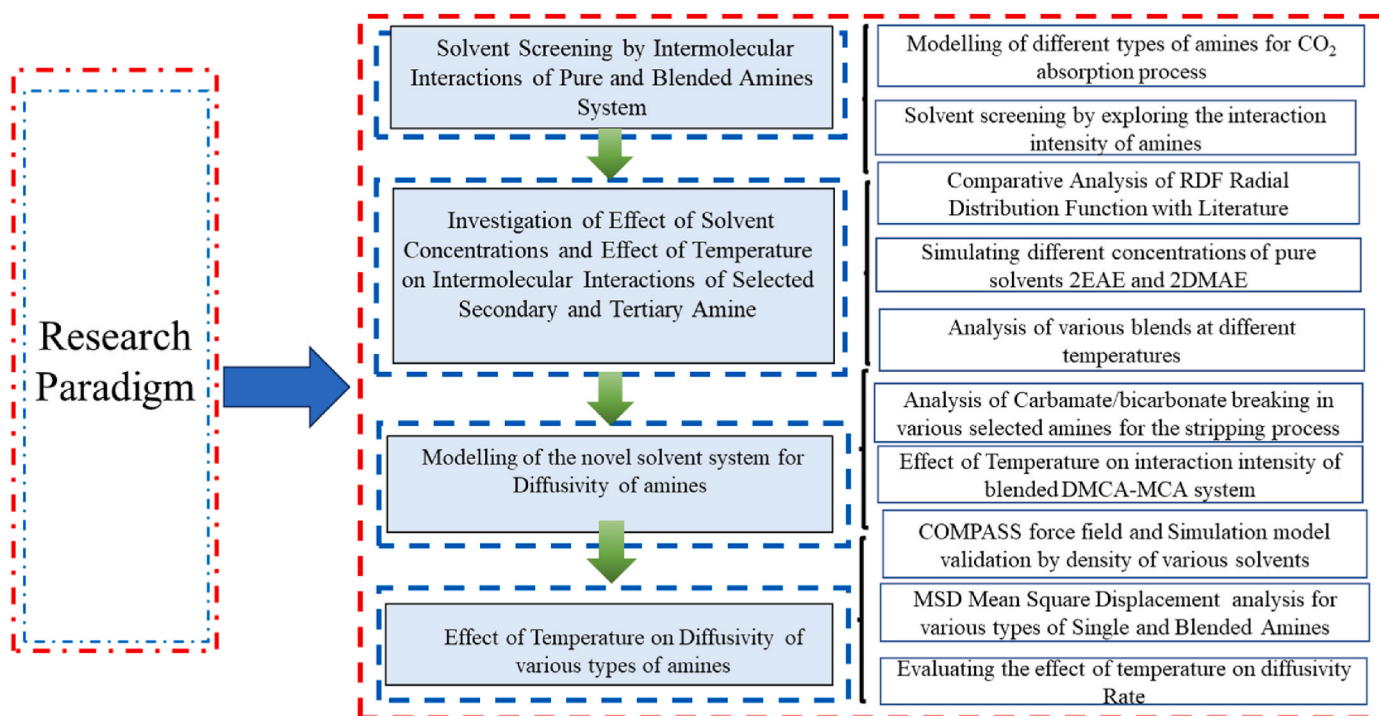


Fig. 3. Conceptual framework for analytical approach in the present work.

Table 2
Attractive and repulsive interactions in various types of amines at 313 K.

Solvent System	$N_{\text{carbamate}^-}$ $C_{\text{carbamate}}$	$N_{\text{carbamate-H}_2\text{O}}(r, g(r))$	$C_{\text{carbamate-O}_2\text{O}}(r, g(r))$
	$H_{\text{bicarbonate}^-}$ $C_{\text{bicarbonate}}$	Attractive Interactions	
	Repulsive Interactions		
TMPAD	1.25, 72	4.75, 1.22	3.75, 0.96
DEAB	1.25, 67	4.25, 1.12	3.75, 0.87
DMCA	1.25, 66	5.25, 0.92	3.75, 1.06
MCA	1.25, 56	4.75, 0.75	3.75, 1.09
2DMAE	1.25, 44	4.75, 1.27	3.75, 1.13
1DMA2P	1.25, 49	4.75, 1.52	4.75, 1.49
2EAE	1.25, 45	4.75, 1.08	3.75, 1.28
AMP	1.25, 47	5.75, 1.09	3.75, 1.24
PZ	1.25, 39	5.75, 0.92	3.75, 0.60
2MAE	1.25, 27	3.25, 1.71	3.75, 1.22
MEA	1.25, 21	4.25, 1.09	3.75, 1.41

of amine categories, including primary, secondary, tertiary, hindered, and cyclic amines. Physical properties of amine solutions for carbon dioxide absorption include increased water solubility and decreased volatility. Alkanolamines, which combine alcohol and amino groups in a single molecule, are commonly used. The hydroxyl group has a significant affinity for water, increasing amine solubility and decreasing surface tension, reducing amine volatility (Yao et al., 2023).

Based on hydrogen substitution at the amino nitrogen, amines are classed as primary, secondary, or tertiary. They can capture CO_2 via a variety of ways. The reactions in Equations (1)–(3) produce carbamate from primary and secondary amines. Unhindered amines, such as monoethanolamine or diethanolamine, produce a powerful carbamate with a fast reaction rate, while subsequent hydrolysis occurs to a lower amount. The carbamate becomes the major product in this case, creating the reaction pathway for secondary and tertiary amines. Because of the methyl group attached to the -carbon atom, hindered amines, such as AMP, prevent CO_2 from interacting stably with the amino group. This

precludes the formation of a stable carbamate, which is the primary consequence of hydrolysis of bicarbonate ion. A free amine molecule is easily liberated and reacts with a new CO_2 molecule. Thus, 1 mol of AMP interacts with 1 mol of CO_2 stoichiometrically. MCA, on the other hand, has an absorption capacity of roughly 1 mol CO_2 /mol amine, which is comparable to the CO_2 capacity of the tertiary amine DMCA (Wang et al., 2021; Zhou et al., 2017).

The graphical representation of RDF results for various selected amines is presented in Fig. 4, which shows that MEA requires highest energy for repulsive attraction as compared to other studied solvents. This is according to the literature, MEA is an excellent choice for absorption phase but has restrictions in the regeneration phase (Damartzis et al., 2016; Caplow, 1968). According to Damartzis et al., 2016, MEA has a strong reactivity with CO_2 (Damartzis et al., 2016). Following MEA, PZ and AMP emerge as promising amine-based absorption candidates. PZ and AMP repulsive interactions exceed MEA by 30.7% and 40%, respectively, showing that PZ and AMP require less energy to break carbamate ion bonds. PZ, in particular, creates bicarbonate ions, and the decomposition of bicarbonate and carbonate requires less energy to break C–O bonds than breaking C–N bonds in carbamate (Kim et al., 2011; Zhao et al., 2024). A strong repulsive interaction suggests that the binding can be disrupted with a minute quantity of heat energy. When AMP and PZ are incorporated into the CO_2 capture mechanism, the amount of heat energy required for amine solvent stripping lowers (Zhang et al., 2016). As a result, PZ and AMP can be used as effective promoters or activators in the amine-based absorption strategy.

2EAE and 2DMAE are two other amines investigated in this study. The secondary amine 2EAE repulsive interactions produce favorable results. The intensity of intramolecular interactions in 2EAE exceeds that of MEA by 40%, implying that 2EAE requires less energy for solvent regeneration than MEA. Due to its increased absorption capacity and quicker reaction kinetics, 2EAE appears as a possible replacement to MEA in the literature (Ahmad et al., 2018). Tertiary amines, such as 2DMAE, often have lesser regeneration energies than primary and secondary amines. The results for 2DMAE show enhanced interaction intensity, indicating that carbamate amine requires less energy for bond breakdown. The increased heat of absorption in primary and secondary

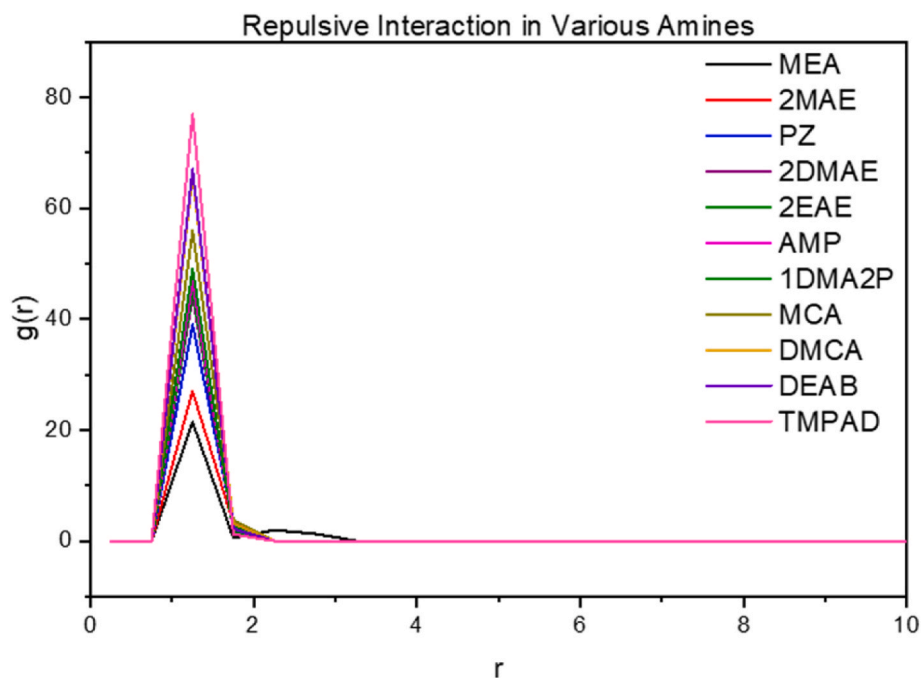


Fig. 4. Graphical representation of RDF (carbamate/bicarbonate) in various types of amines.

amines due to carbamate synthesis adds to higher regeneration energy. Tertiary amines, on the other hand, require less energy to regenerate. Furthermore, tertiary amines have a slow reaction rate, leading suggestions for mixing with secondary amines. Moreover, while comparing to MEA, MCA has a 51% increase in intramolecular interaction intensity. MCA, according to the research, acts as an effective promoter, greatly increasing CO₂ absorption rates and capacities (Zhou et al., 2017). Notably, MCA has a low toxicity, making it reasonably safe for both human health and the environment. In the context of a possible amine for CO₂ capture, DMCA has the highest intramolecular interaction intensity, implying that carbamate bond breakdown requires little heat. Existing research shows that, as compared to other tertiary amines, DMCA has a high cycle capacity and a fast regeneration rate (Ye et al., 2015). DMCA has a stronger repellent impact than MEA, with a repulsive interaction strength that is roughly 59% higher.

Following in the pattern of DMCA, the tertiary amine DEAB demonstrates a strong repulsive effect (1.25, 67). According to the literature, DEAB has a higher absorption capacity and a higher cycling capacity, which can effectively reduce the circulating rate in a packed column (Naami et al., 2012). The strong repelling effect found in this work with DEAB shows that breaking the H-C bond in bicarbonate molecule is simple, requiring less energy for solvent regeneration than MEA (Sema et al., 2011). TMPAD, being a diamine, exhibits the most pronounced intensity for repulsive interaction. The sequence of regeneration energy needed to break the carbamate or bicarbonate in various selected amines, ranked from lower higher to is TMPAD < DEAB < DMCA < MCA < 1DMA2P < AMP < 2EAE < 2DMAE < PZ < 2MAE < MEA. In conclusion, tertiary amines exhibit higher repulsive interactions owing to steric hindrance produced by the presence of bulky groups. Furthermore, the current study's findings on the repulsive interaction of MEA exhibits enhanced stability of the carbamate ion, posing a greater challenge to bond rupture compared to other amines investigated in this research. As a result, in the given context, TMPAD requires the least amount of energy for solvent regeneration, while MEA requires the most.

3.2. Effect of solvent concentration on CO₂ absorption for various types of amines at 313 K

In this study, different concentrations were explored to optimize solvent efficiency for CO₂ capture, deviating from the commonly used 30% MEA. Various single and blended amines, including 2EAE, 2DMAE, 2EAE-PZ, 2DMAE-PZ, and DMCA-MCA, were assessed for interaction intensity at temperatures between 40 °C and 60 °C. Table 3 summarizes the findings of the DMCA/MCA blend at different concentrations. From Table 3 it can be seen that the interaction with water (N_{DMCA-H_2O} & N_{MCA-H_2O}) are highest in the 30% DMCA-10% MCA mixture, which highlights the improved solubility of DMCA-MCA blend in H₂O. On the other side $N_{amine-CO_2}$ has a stronger intermolecular interaction in 10% DMCA-20%MCA. The stronger intensity with CO₂ indicates high reactivity of this blend to CO₂.

Overall, the data indicates that optimizing the blend by reducing DMCA while increasing MCA concentration enhances intermolecular interactions. The 10% DMCA-20% MCA blend exhibits the highest intermolecular interaction strength compared to other concentrations. Significant interactions between N_{DMCA} and C_{CO_2} in this blend suggest increased CO₂ reactivity. These findings align with prior research for example Wang et al., 2019, explored DMCA-MCA blends with various concentrations and found that the DMCA-MCA blend with the highest MCA concentration (1 M–3M), exhibited superior absorption rates compared to 5MMEA in a comprehensive range (Wang et al., 2021). Notably, MCA (N-methylcyclohexylamine), has been identified as an activator in previous studies (Zhang et al., 2011, 2013, 2018; Ye et al., 2015). The observed trend in our study supports the notion that optimizing MCA concentration plays a crucial role in enhancing

Table 3
Interactions of DMCA-MCA blend at 313 K.

DMCA-MCA	N_{MCA-CO_2}	N_{MCA-H_2O}	N_{DMCA-H_2O}	$N_{DMCA-CO_2}$
10%–20%	5.25, 1.29	4.75, 0.80	4.75, 0.88	4.75, 1.85
20%–10%	5.25, 1.21	4.75, 0.77	4.75, 0.85	4.75, 1.46
30%–10%	5.25, 1.46	4.75, 0.88	4.75, 0.90	4.75, 1.35

C_{CO_2} =Carbon of CO₂, H_{H_2O} =Hydrogen in H₂O N_{MCA} =Nitrogen of MCA, N_{DMCA} =Nitrogen of DMCA.

intermolecular interactions within DMCA-MCA blends. It's evident that strategic adjustments in the DMCA-MCA ratio can significantly impact the absorption performance, emphasizing the importance of tailored blend compositions for optimal results in carbon capture technologies.

The other screened solvent is 2EAE. Table 4 summarize the findings for 2EAE, focusing on specific interactions such as $N_{2EAE-H_{water}}$, $HO_{2EAE-O_{water}}$, $O_{2EAE-CO_2}$ and $N_{2EAE-CO_2}$. The distance beyond 15 Å as negligible. In the 2EAE system, the intermolecular interactions $N_{2EAE-H_{water}}$ and $HO_{2EAE-O_{water}}$ exhibit strengths of 1.08 at 4.75 Å and 1.23 at 2.25 Å, respectively, for a 30% solvent concentration. At 40% concentration, the strength at 4.75 Å increases to 1.14, and further concentration increments (50% and 60%) result in strengths of 1.19 and 1.24, respectively. Similar concentration-dependent patterns are observed in $HO_{2EAE-O_{water}}$ and $N_{2EAE-H_{water}}$ interactions, rises from 30% to 60%, suggesting higher solubility due to stronger interactions with the hydroxyl group. It indicates increased interaction strength with higher concentrations. However, this trend is opposite in $O_{2EAE-CO_2}$ interaction. The intensity decreases with increasing concentration, reaching its lowest at 60%, implying a weaker effect at higher concentrations. Similarly, for $N_{2EAE-CO_2}$ interactions, the strength decreases from 1.41 at 30% concentration to 1.28 at 40% concentration, again it increases to 1.32 and 1.37 at 50% and 60% concentrations, respectively. These trends indicate that for 2EAE, the maximum strength is in 30% of 2EAE as the most important interactions $N_{2EAE-CO_2}$ & $O_{2EAE-CO_2}$ show highest tendency at 30%2EAE.

Table 5 compares the interactions at different solvent concentrations for 2DMAE, demonstrating increased intermolecular interaction strength for $N_{2DMAE-H_{water}}$ and $HO_{2DMAE-O_{water}}$ interactions with rising solvent percentages. At 4.75 Å, $N_{2DMAE-H_{water}}$ exhibits strengths of 1.25 Å, 1.37 Å, 1.42 Å, and 1.47 Å for 30%, 40%, 50%, and 60% concentrations, respectively. Similarly, $HO_{2DMAE-O_{water}}$ interactions show strengths of 1.31 Å, 1.41 Å, 1.60 Å, and 1.77 Å for the corresponding concentrations, indicating heightened responsiveness of hydroxyl and amino groups to CO₂ in water. $O_{2DMAE-CO_2}$ interactions increase in strength from 1.11 at 30% to 1.17 at 60%, with a 5.12% increment, while reducing to 1.08 at 50% concentration. $N_{2DMAE-CO_2}$ interactions exhibit strengths of 1.75 and 1.80 at 5.25 Å for 30% and 40%, and 1.75 and 1.81 for 50% and 60%, indicating consistent intensities. Contrarily, $N_{2DMAE-H_{water}}$ and $HO_{2DMAE-H_{water}}$ interactions show a stronger tendency at 50% and 60% 2DMAE concentrations, with comparable results at 40%. The lack of noticeable improvement in interactions between $O_{2DMAE-CO_2}$ and $N_{2DMAE-CO_2}$ suggests a slower reaction of the tertiary amine to acidic gas. However, the other two interactions indicate that 2DMAE, as a tertiary amine, exhibits higher water solubility. Literature supports this finding, as tertiary amines are generally less reactive compared to primary and secondary amines (Ciftja et al., 2013). Table 5 highlights that, at a 40% solvent concentration, all observed interactions exhibit the maximum g(r). As a result, the findings indicated that 40% of 2DMAE and 30% of 2EAE and yield a better performance for faster CO₂ absorption process. These results can be justified with other studies (George et al., 2020; Vega et al., 2018), which explored the secondary and tertiary amines for CO₂ capture application and results of this study indicates 30% for secondary amines and up to 60% of tertiary amines can be suitable for CO₂ absorption process. Similarly, the experimental study explored the effect of amine

Table 4
RDF results for 2EAE at various concentrations at 313 K.

2EAE	$N_{2EAE-CO_2}$	$O_{2EAE-CO_2}$	$HO_{2EAE-O_{water}}$	$N_{2EAE-H_{water}}$
60%	5.25, 1.37	5.25, 1.15	3.25, 1.79	4.75, 1.24
50%	5.25, 1.32	5.25, 1.16	3.25, 1.62	4.75, 1.19
40%	4.75, 1.28	5.25, 1.16	3.25, 1.40	4.75, 1.14
30%	5.25, 1.41	5.25, 1.19	2.25, 1.32	4.75, 1.08

HO_{2EAE} =Hydrogen at oxygen in 2EAE, O_{2EAE} =Oxygen of 2EAE, CO_2 =Carbon of CO₂, H_{water} = Hydrogen of water, N_{2EAE} =Nitrogen in 2-(ethylamino) ethanol.

Table 5
RDF results of 2DMAE at Various Concentration at 313 K.

2DMAE	$N_{2DMAE-CO_2}$	$O_{2DMAE-CO_2}$	$HO_{2DMAE-O_{H_2O}}$	$N_{2DMAE-H_{Water}}$
60%	5.25, 1.81	5.25, 1.17	3.25, 1.77	4.75, 1.47
50%	5.25, 1.75	5.25, 1.08	3.25, 1.60	4.75, 1.42
40%	5.25, 1.80	5.25, 1.19	3.25, 1.41	4.75, 1.37
30%	5.25, 1.75	5.25, 1.11	3.25, 1.31	4.75, 1.25

O_{2DMAE} =Oxygen of 2DMAE, CO_2 =Carbon of CO₂, HO_{2DMAE} =Hydrogen at oxygen in 2DMAE, H_{water} = Hydrogen of water, N_{2DMAE} =Nitrogen in 2-dimethylamino ethanol.

concentration and amine circulation rate on the removal of CO₂. The result of this study indicates that increasing the solvent concentration, the net acid gas loading decreases (George et al., 2020; Vega et al., 2018). This is because viscosity influences absorption. Because the rate of CO₂ absorption is governed by mass transfer resistance in the liquid, the more viscous the solution, the greater the amine's resistance to absorb acid gases. This indicates that, after a certain limit, we cannot increase the amine concentration because it causes the increase in viscosity which causes foaming and reduces the loading.

Table 6 presents an analysis of varying percentages of 2EAE and 2DMAE with PZ. The results indicate increased intermolecular interaction strength with PZ concentration, particularly in hydrogen bonding with water. The interactions with CO₂ remain relatively unaffected by PZ, with the highest interaction strength observed at 30% PZ-10% 2EAE and 313 K. Parallel to this, analysis of different 2DMAE percentages shows that PZ-2DMAE hydrogen bonding interactions are more water soluble than PZ-2EAE blend at 313 K (Table 6). It is noteworthy that interactions with CO₂ do not exhibit a regular pattern when PZ concentration increases. This is likely due to the complicated structure of the tertiary amine 2DMAE. PZ does increase interaction strength; the increment is modest. Table 6 shows that 15%PZ-15%2DMAE has the highest interaction intensity among the concentrations under investigation, regardless of intensity variations.

Table 7 compares the 2EAE-PZ blend (30%2EAE-10%PZ) and the 30%PZ-10%2EAE blend with DEA (Sharif et al., 2020). In comparison to the current investigation, the $N_{2EAE-H_{H_2O}}$ and $HO_{2EAE-O_{H_2O}}$ interactions exhibit larger values in 2EAE-PZ and DEA. Even though they are secondary amines, the greater interaction in 2EAE-PZ points to better water solubility, which is consistent with research showing that 2EAE is more CO₂ soluble than 2DMAE (Muchan et al., 2017). While the $O_{2EAE-CO_2}$ interaction is most prominent in 30%PZ-10%2EAE, suggesting increased reactivity of 2EAE with CO₂ emphasizing the amine's effectiveness in reacting with acidic gas. The $N_{2EAE-CO_2}$ interaction behaves equally for both secondary amines DEA and 2EAE. The findings overall support the use of piperazine blends to improve absorption capacity and reaction rates, particularly 30%2EAE-10%PZ, to boost reaction rates and absorption capacity. In comparison, pure 2EAE demonstrates higher interaction intensity than DEA, establishing the order of intermolecular strength as 30%2EAE-10%PZ > 30%PZ-10%2EAE, and 2EAE > DEA. The graphical representation of RDF comparison with literature is provided in Supplementary material in Figure S1 to Figure S5.

Moreover, the study also compares the findings of PZ-2DMAE with MDEA-PZ and 2DMAE-PZ (Sharif et al., 2020; Harun et al., 2017b), detailed in Table 7. The analysis of intermolecular interaction intensity indicates that 2DMAE-PZ exhibits the highest interaction intensity compared to pure 2DMAE and PZ-2DMAE, suggesting that a small amount of piperazine is more favorable. MDEA-PZ shows the highest interactions among all blends, emphasizing PZ's role as an effective promoter due to its rapid carbamate formation with CO₂ (Idem et al., 2009; Bishnoi et al., 2000). The lower intermolecular interaction of 2DMAE is attributed to its structure with two methyl groups and one ethanol group at the nitrogen atom, reducing amine reactivity with CO₂ (Idris et al., 2014). On the other side, MDEA lacking a hydrogen atom in the amino group, prevents it from directly reacting with CO₂. PZ acts as a

Table 6

Radial Distribution Function analysis of PZ-2EAE and PZ-2DMAE at 313 K.

PZ-2EAE	N _{PZ} -C _{CO2}	N _{PZ} -H _{H2O}	N _{2EAE} -C _{CO2}	O _{2EAE} -C _{CO2}	HO _{2EAE} -O _{H2O}	N _{2EAE} -H _{H2O}
10%–20%	5.25,1.33	4.75,0.91	5.25,1.30	5.25,1.12	3.25,1.27	4.75,1.03
15%–15%	5.25,1.40	5.25,0.87	5.25,1.32	4.75,1.07	3.25,1.32	4.75,1.03
20%–10%	5.25,1.19	4.75,0.92	5.25,1.47	3.25,1.00	3.25,1.26	4.75,1.02
30%–10%	5.25,1.12	4.75,0.94	5.25,1.40	3.25,1.42	3.25,1.47	4.75,1.13
PZ-DMAE	N _{PZ} -C _{CO2}	N _{PZ} -H _{H2O}	N _{DMAE} -C _{CO2}	O _{DMAE} -C _{CO2}	HO _{DMAE} -O _{H2O}	N _{DMAE} -H _{H2O}
10%–20%	5.25,1.38	4.75,0.93	4.75,1.55	5.25,1.05	3.25,1.30	4.75,1.23
15%–15%	5.25,1.34	5.25,0.96	4.75,1.78	5.25,1.01	3.25,1.32	4.75,1.25
20%–10%	5.25,1.38	4.75,0.87	5.25,1.65	3.25,0.94	3.25,1.30	4.75,1.16
30%–10%	5.25,1.25	4.75,0.95	4.75,1.76	3.25,1.10	3.25,1.41	4.75,1.25

N_{2EAE}=Nitrogen in 2ethylamino ethanol, H_{H2O}=Hydrogen of water, C_{CO2}= Carbon of CO₂, O_{2EAE}= Oxygen of 2EAE, HO_{2EAE}=Hydrogen at oxygen in 2EAE.**Table 7**

Comparisons of results with literature for 2EAE and 2DMAE.

Solvent	N _{PZ} -C _{CO2}	N _{PZ} -H _{H2O}	N _{2EAE} -C _{CO2}	O _{2EAE} -C _{CO2}	HO _{2EAE} -O _{H2O}	N _{2EAE} -H _{H2O}	Reference
2EAE	–	–	5.25, 1.41	5.25, 1.19	2.25, 1.32	4.75, 1.08	Sharif et al. (2023b)
2EAE-PZ	4.75, 1.07	5.75,1.09	5.25, 1.43	4.75, 1.30	3.25, 1.69	4.75, 1.08	Sharif et al. (2020)
PZ-2EAE	5.25, 1.40	5.25, 0.87	5.25, 1.32	4.75, 1.07	3.25, 1.32	4.75, 1.03	Sharif et al. (2020)
DEA	N _{PZ} -C _{CO2}	N _{PZ} -H _{H2O}	N _{DEA} -C _{CO2}	O _{DEA} -C _{CO2}	HO _{DEA} -O _{H2O}	N _{DEA} -H _{H2O}	
–	–	–	5.25, 1.42	3.75, 1.13	5.75, 1.59	5.75, 1.01	
DMAE	N _{PZ} -C _{CO2}	N _{PZ} -H _{H2O}	N _{DMAE} -C _{CO2}	O _{DMAE} -C _{CO2}	HO _{DMAE} -O _{H2O}	N _{DMAE} -H _{H2O}	
–	–	–	5.25, 1.75	5.25, 1.11	2.25, 1.31	4.75, 1.25	Sharif et al. (2020)
PZ-DMAE	5.25, 1.34	5.25, 0.96	4.75, 1.78	5.25, 1.01	3.25, 1.32	4.75, 1.25	
DMAE-PZ	5.75, 1.41	5.25, 0.97	5.25, 1.79	5.25, 1.15	3.25, 1.41	4.75, 1.28	Sharif et al. (2020)
MDEA-PZ	N _{PZ} -C _{CO2}	N _{PZ} -H _{H2O}	N _{MDEA} -C _{CO2}	O _{MDEA} -C _{CO2}	HO _{MDEA} -O _{H2O}	N _{MDEA} -H _{H2O}	
5.25, 1.49	5.75, 1.15	5.25 1.87	3.75, 1.18	1.75, 2.70	4.75, 1.88		Masiren et al. (2016a)

PZ= PZ + CO₂+H₂O, 2EAE = 2EAE + CO₂+H₂O, 2EAE-PZ = 30%2EAE-10%PZ, PZ-2EAE = 30%PZ-10%2EAE, DEA PZ = DEA + PZ + CO₂+H₂O.

promoter, facilitating the rapid transfer of CO₂ to MDEA (Lu et al., 2005). Therefore, the order of intermolecular interaction strength is MDEA-PZ > 2DMAE-PZ > PZ-2DMAE > 2DMAE. These results can be verified by experimental studies in literature. For example, the study conducted by Mudhasakul et al., 2013 shows that increasing the concentration of piperazine, increases the CO₂ absorption process but at certain limit, the increase in piperazine concentrations does not lead to favorable results. Finally, only 5% of PZ was considered the best concentration with 45%MDEA (Mudhasakul et al., 2013). Similar results were obtained by (Ibrahim et al., 2014) that lower concentration of piperazine show better performance. In fact, there are numerous experimental investigations in the literature that show the addition of PZ to amine solution as a rate promotor or activator (Du et al., 2016; Freeman et al., 2012). Unlike this research, we used the molecular dynamic simulation model. The findings of the current research and other studies in the literature are consistent. As a result, we can say that these investigations can aid in validating the simulation results of the current study. The summary of the findings is presented in Table 8.

Table 8

Solvent concentration optimization in the present work.

Name	Concentrations of solvent	Effect of Concentration on Intensity	Temperature effect on Diffusivity
2EAE	30%	–	The diffusivity of solvents increases by increasing the temperature
2EAE-PZ	30%–10%	A lower concentration of PZ shows higher interaction intensity for blended	
2DMAE-PZ	30%–10%	2EAE and 2DMAE	
PZ-2EAE	30%–10%		
PZ-2DMAE	15%–15%		
2EAE	30%	30% of a Secondary amine	
2DMAE	40%	40% of Tertiary amine	
DMCA-MCA	10%–20%	10%DMCA-20%MCA	

Author's Tabulation.

DMCA-MCA, DEAB, 2DMAE, MEA, 2EAE, 2MAE, 1DMA2P, and TMPAD have been carefully selected for analysis. The findings have been interpreted through Mean Square Displacement analysis as presented in Fig. 5.

Table 9 shows the diffusion coefficient results of various selected amines. Various types of amine blends are observed. Two secondary amines 2EAE and 2MAE are selected to blend with tertiary amines i.e., 2EAE-TMPAD, 2EAE-1DMA2P, 2EAE-DEAB and 2MAE-TMPAD, 2MAE-1DMA2P, 2MAE-2DMAE and 2MAE-DEAB. The diffusion coefficient outcomes for different blends indicate that the 2MAE-DEAB mixture exhibits a greater diffusion rate compared to the 2MAE-TMPAD, 2MAE-2DMAE, and 2MAE-1DMA2P blends. 2MAE, a secondary amine, exhibits compatibility for blending with 2DMAE. Secondary amines are deemed potential solvents for CO₂ absorption, given their amine functionality facilitating reactions with CO₂ to form carbamate compounds. The properties of 2DMAE underscore its high loading capacity, low absorption heat, and reasonable reaction rate (Idris et al., 2014). Notably, the diffusivity results for 2DMAE reveal that the diffusion rate in pure 2DMAE exceeds that observed in blended systems (Idris et al., 2014). Tertiary amines typically exhibit slow reaction rates, and diffusivity is intricately linked to reaction kinetics, where elevated diffusivity implies a solvent with heightened kinetics. Literature supports the notion that tertiary amines generally manifest slower reaction rates compared to primary and secondary amines. The relatively low diffusivity rate of 2DMAE may stem from its structural characteristics, including the substitution of a methyl group with a dimethyl group and alcohol substitution on the nitrogen atom, both of which contribute to reduced reactivity towards CO₂ (Idris et al., 2014).

The diffusion coefficient analysis of 2EAE blends reveals that 2EAE-TMPAD exhibits the highest diffusion rate among blends, surpassing 2EAE-DEAB and 2EAE-1DMA2P. Tertiary amines, including 1DMA2P and DEAB, show noteworthy diffusion rates when paired with 2EAE. Notably, 1DMA2P shares characteristics with other tertiary amines, such as DEAB and 2DMAE, with lower absorption heat than 2DMAE. The diffusion coefficients for the blended system 2EAE-1DMA2P align with those observed in other combinations. Moreover, 2EAE-TMPAD and 2EAE-DEAB demonstrate similar diffusivity, showcasing DEAB's promising attributes as a CO₂ absorption candidate, including high cyclic

Table 9

Comparison of CO₂ diffusivity estimation from present work and literature at 313 K.

Solvent	Diffusivity (D_{CO_2})/m ² s ⁻¹	References
MEA	2.11E-09	Sharif et al. (2022)
2EAE	3.44E-09	Sharif et al. (2022)
2MAE	0.50E-09	Sharif et al. (2023a)
2DMAE	1.70E-09	Sharif et al. (2022)
DEAB	0.63E-09	Sharif et al. (2023a)
1DMA2P	0.53E-09	Sharif et al. (2023a)
TMPAD	0.68E-09	Sharif et al. (2023a)
2MAE-TMPAD	0.91E-09	Sharif et al. (2023a)
2MAE-DEAB	1.29E-09	Sharif et al. (2023a)
2MAE-1DMA2P	1.02E-09	Sharif et al. (2023a)
MEA-PZ	0.53E-09	Sharif et al. (2023a)
AMP-PZ	0.92E-09	Sharif et al. (2023a)
	0.92E-09	Khan et al. (2019)
MEA-AMP	0.65E-09	Khan et al. (2019)
2EAE-TMPAD	0.98E-09	Sharif et al. (2020)
2EAE-DEAB	0.98E-09	Sharif et al. (2020)
2EAE-1DMA2P	0.84E-09	Sharif et al. (2020)
DMCA-MCA	0.61E-09	Sharif et al. (2023a)
	0.63E-09	(Wang et al., 2019, 2021)

capacity and low heat of absorption. The order of diffusion rates in 2EAE blends is 2EAE-TMPAD > 2EAE-DEAB > 2EAE-1DMA2P > 2EAE-2DMAE. Other three blends investigated in the study are MEA-PZ, AMP-PZ, and MEA-AMP. Mean Square Displacement (MSD) graphs at three distinct temperatures (298 K, 308 K, and 318 K) are shown in the supplementary material (Figure S5 and S6). The diffusion coefficient is found to have a linear relationship, which shows that it consistently increases with temperature and time. Table 9's results demonstrate that the diffusivity of the AMP-PZ blend is higher than that of the MEA-PZ and MEA-AMP blends.

Both AMP and PZ are recognized as effective promoters in the literature. Additionally, Table 10 illustrates that with increasing temperature, the diffusion coefficient values rise, with the highest diffusivity observed at 313 K, followed by 298 K and 308 K. This temperature-dependent increase in diffusivity is attributed to the elevated kinetic energy of molecules, leading to enhanced particle collisions. Table 10

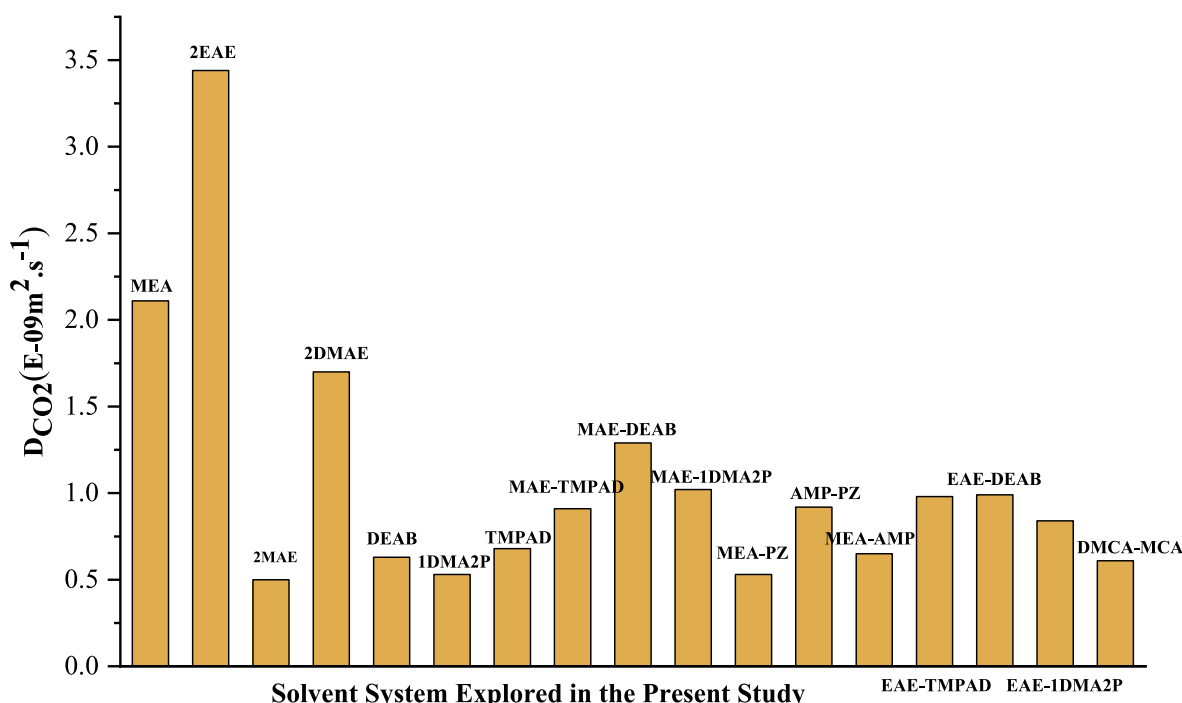


Fig. 5. CO₂ Diffusivity (E-09 m² s⁻¹) Estimation in Various amines at 313 K.

Table 10
Comparison of diffusivity prediction in AMP-PZ between present study and literature.

System	Present study (DCO ₂)/m ² . s ⁻¹	Experimental studies (DCO ₂)/m ² . s ⁻¹	Deviation (%)	Temperature/K	References
CO ₂ in AMP-PZ	0.59E-09	0.52E-09	13.46	298	Khan et al. (2019)
	0.77E-09	0.75E-09	2.67	308	Khan et al. (2019)
	0.92E-09	0.92E-09	0	313	Khan et al. (2019)
CO ₂ in MEA	1.40E-09	1.40E-09	0	298	Sharif et al. (2022)
	2.11E-09	2.11E-09	0	313	Masiren et al. (2016b)
	2.41E-09	2.42E-09	0.41	318	Masiren et al. (2016b)

also provides insights into the deviation between our predicted diffusivity values and the corresponding experimental values at each temperature for both CO₂ in AMP-PZ and CO₂ in MEA systems. It appears that in most cases, the deviations are relatively small, indicating a reasonably good agreement between our predictions and experimental observations.

2-amino-2-methyl-1-propanol (AMP), acknowledged for its higher absorption capacity and energy-efficient regeneration compared to MEA, has gained prominence. Combining PZ and AMP is anticipated to synergize their positive characteristics while overcoming any drawbacks (Khan et al., 2019). The present study focuses on the diffusion coefficient of the AMP-PZ blend, aiming to provide insights into the kinetics of aqueous AMP-PZ, a fundamental aspect for efficient plant design. Comparisons with the benchmark MEA reveal that MEA exhibits higher diffusivity than AMP-PZ (Table 10).

According to (Dey et al., 2009), higher diffusivity corresponds to faster reaction kinetics. The study aligns with existing literature, indicating MEA's superior reaction kinetics but highlighting the challenge of higher regeneration energy in the desorption process. The carbamate stability results also support these findings that AMP-PZ requires less energy for carbamate breakage during regeneration, suggesting a more energy-efficient regeneration process for the AMP-PZ blend. The analysis of diffusivity data for AMP-PZ was conducted in comparison with experimental results documented in the literature, as outlined in Table 10 and Fig. 6.

Furthermore, Table 11 offers an extensive examination of various attributes of different amines utilized in CO₂ absorption processes, covering factors such as CO₂ loading capacity, heat of absorption, heat of desorption, and diffusion coefficient. Among the investigated amines,

TMPAD demonstrates the highest CO₂ loading capacity, indicating its potential for effective CO₂ capture. These results are according to our findings that TMPAD can be a potential candidate for CO₂ capture application. Furthermore, Table 11 outlines the heat of reaction for each amine solvent, shedding light on the energy demands of the CO₂ absorption process. Hindered amines exhibit notable absorption rates and effective stripping performance, but are hindered by challenges such as heightened viscosity and increased heat retention. To overcome the challenge of high viscosity, strategies involve reducing water concentration or introducing organic solvents.

On the other side, tertiary amines show promise in loading capacity and reduced heat retention, yet they face limitations such as lower absorption rates and higher viscosity. Overcoming these hurdles necessitate the implementation of temperature regulation or catalysts to moderate reaction kinetics and enhance overall process efficiency. Traditionally, the combination of tertiary amines with primary or secondary amines has been a common practice, leveraging the faster reaction rates of the latter, while still capitalizing on the benefits of high loading capacity, low solvent degradation, and cost-effective regeneration (Mudhasakul et al., 2013). However, the inherent slow reaction rate of tertiary amines can pose challenges, potentially leading to increased capital costs in gas sweetening units, as the absorption column necessitates numerous theoretical steps. Consequently, tertiary amines exhibiting both high loading capacity and fast reaction rates are deemed highly desirable.

Secondary amines offer elevated CO₂ absorption capacity and decreased corrosiveness compared to primary amines, yet they too encounter challenges such as higher viscosity, corrosiveness, and restricted water solubility. Potential solutions include exploring solvent

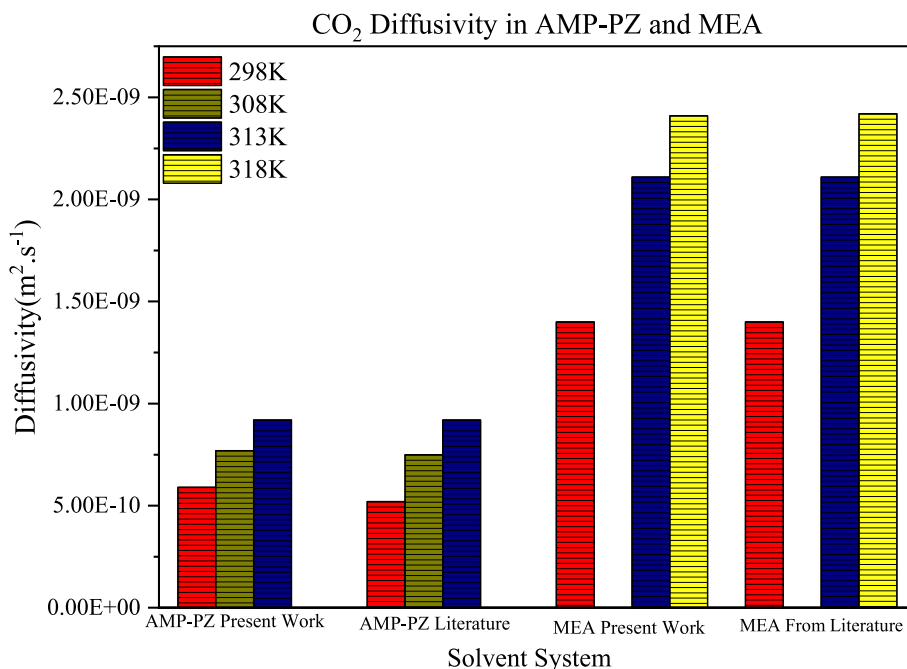


Fig. 6. Comparison of CO₂ diffusivity in AMP-PZ and MEA with literature (Sharif et al., 2022; Khan et al., 2019; Masiren et al., 2016b).

Table 11
Properties of Amines from Present work and Existing Literature.

Solvents	CO ₂ Loading (molCO ₂ /mol amine)	Heat of Absorption ($\Delta H =$ kJmol ⁻¹ of CO ₂) (El Hadri et al., 2017)	Heat of Desorption ($\Delta Q_{reg} =$ kJmol ⁻¹ of CO ₂) (Singto et al., 2016)	Diffusion Coefficient DCO ₂ (m ² s ⁻¹) at 313 K Present Work	Reference
MEA	0.55	55	175.72	2.11E-09	El Hadri et al. (2017)
2EAE	0.71	51	86.65	1.47E-09	(Sharif et al., 2022; Muchan et al., 2017)
2DMAE	0.77	45	60.84	1.40E-09	Sharif et al. (2022)
2MAE	0.67	73.83	n/a	0.50E-09 (this work)	(Sharif et al., 2022; Muchan et al., 2017)
AMP	0.73	50	58.30	n/a	Muchan et al. (2017)
DEAB	0.59	41	54.37 (Singto et al., 2016)	0.68E-09	(Sharif et al., 2022; Sema, 2012)
TMPAD	1.32	59.87	n/a	0.68E-09 (this work)	El Hadri et al. (2017)
1DMA2P	0.83	30	n/a	0.53E-09 (this work)	(Kadiwala et al., 2012; El Hadri et al., 2017; Liang et al., 2015)
PZ	1.25	70	n/a	2.15E-09 (Sharif et al., 2024)	Liang et al. (2015)
AMP	0.94	73	n/a	n/a	Muchan et al. (2017)

Characteristics and Drawbacks of Various Types of Amines					
Solvent Group	Example	Heat of Reaction (MJ/kg CO ₂) (Raksajati et al., 2018)	Characteristics	Drawback of Solvent	Reference
Polyamines	C ₄ H ₁₀ N ₂ (PZ)	66–78	Enhances reaction rate Antioxidative Prevents thermal degradation	Restricted solubility in water Absorption of CO ₂ and water from air	Van Wagener et al. (2011)
Hindered amines	HN-CH-(CH ₃) ₂ -CH ₂ -OH (AMP)	50–75	Significant absorption rate Sufficient loading capacity Excellent stripping performance	Elevated viscosity Costly	(Choi et al., 2009; Neveux et al., 2013)
Tertiary amine	C ₆ H ₁₁ N(CH ₃) ₂ (DMCA) CH ₃ CH(OH)CH ₂ N(CH ₃) ₂ (1DMA2P) TMPAD (CH ₃) ₂ N(CH ₂) ₃ N(CH ₃) ₂ DEAB C ₈ H ₁₉ NO	50–65	Sufficient loading capacity Reduced heat capacity Moderated vapor pressure Decreased heat of reaction	Reduced absorption rate Costly Higher viscosity	(Rangwala et al., 1992; Xiao et al., 2000)
Secondary amines	(CH ₃) ₂ NCH ₂ CH ₂ OH (2DMAE) CH ₃ -NH-CH ₂ -CH ₂ -OH (2MAE) C ₆ H ₁₁ NH-CH ₃ (MCA) C ₂ H ₅ NHCH ₂ CH ₂ OH (2EAE)	65–75	Elevated CO ₂ absorption capacity Reduced heat capacity Decreased vapor pressure Lower heat of reaction Less corrosive compared to MEA	Higher viscosity Corrosiveness Limited water solubility	(Gao et al., 2019; Adeosun et al., 2013)
Primary amines	H ₂ N-CH ₂ -CH ₂ -OH (MEA)	70–85	High absorption efficiency Reduced Viscosity Cost-effective	Elevated Heat Capacity Higher Vapor Pressure Costly Regeneration Process	Vaidya et al. (2007)

modifications like blending secondary amines with tertiary amines, utilizing corrosion-resistant materials, optimizing operational parameters to minimize corrosion risks, and enhancing diffusivity to facilitate faster CO₂ absorption and desorption rates (Muchan et al., 2017; Naami et al., 2012). This present study is an effort to overcome these hurdles by suggesting various solvent blends. Further details on the findings of the present work are provided as Table S4 in the supplementary materials.

Our findings indicate that the blended amine system demonstrated the highest diffusion rate for 2MAE- DEAB followed by 2MAE-1DMA2P, 2EAE-DEAB, and 2EAE-TMPAD. While in single amine solvent 2EAE followed MEA, and 2DMAE shows highest diffusivity rate as compared to other selected amines. This comprehensive examination provides valuable insights into the performance and constraints of different amine solvents, aiding in their selection for CO₂ capture applications and guiding further research and optimization endeavors.

4. Conclusion

A molecular dynamic simulation model is developed in Material studio to compute the inter and intra-molecular interaction intensity between various single and blended solvent system (i.e., TMPAD, DEAB, DMCA, MCA, 1DMA2P, AMP, 2EAE, 2DMAE, PZ, 2MAE and MEA). The effect of operating variables like temperature and solvent concentration

on interaction intensity is also analysed. The diffusion coefficient of CO₂ in EAE, MEA, DMAE, MAE-DEAB, MAE-DMA2P, EAE-TMPAD, AMP-PZ, EAE-DEAB, MAE-TMPAD, EAE-DMA2P, MAE-DMAE, EAE-DMAE, TMPAD, MEA-AMP, DMA2P, DMCA-MCA, DEAB, and MEA-PZ is also estimated. The results of the present study are as follows,

- The desorption stage stands out as the most costly segment in the absorption process due to the elevated temperatures needed to rupture the amine-CO₂ bond. A range of amines, including MEA, 2MAE, PZ, 2DMAE, 2EAE, AMP, 1DMA2P, MCA, DMCA, DEAB, and TMPAD, underwent simulation to determine the intra-molecular interaction intensity during the CO₂ desorption process. The findings concerning interaction intensity indicate that N, N, N', N'-Tetramethylpropane-1,3-diamine (TMPAD), N-dimethylcyclohexanamine (DMCA), and 4-diethylamino-2-butanol (DEAB) displayed a tendency for more accessible bond breakage compared to other amines. This suggests that TMPAD, exhibiting the highest repulsive interaction, necessitates the least energy to rupture the carbamate ion/bicarbonate and separate CO₂ during the stripping process in comparison to MEA. The order of energy required to rupture the N-C/H-C bond in the chosen amines, from to lowest highest, is as follows: TMPAD <

DEAB < DMCA < MCA < 1DMA2P < AMP < 2EAE < 2DMAE < PZ < 2MAE < MEA.

- (b) The effect of concentrations on interaction intensity results revealed that the most substantial intermolecular interactions with CO₂ are observed in the case of 30 wt% 2EAE and 40 wt% 2DMAE. While observing the effect of piperazine in the secondary and tertiary amines, it is seen that 30%PZ-10%2EAE and 15% of piperazine-15%2DMAE show higher intermolecular interaction strength as compared to other concentration blends. The relatively high intermolecular interaction demonstrates that particular concentrations for 2EAE and 2DMAE are more reactive to CO₂ and can increase the absorption process. In addition, the examination of the DMCA-MCA blended system reveals that the combination of 10% DMCA and 20% MCA demonstrates superior interaction strength in contrast to other concentration ratios. These optimal concentrations of particular solvents can improve the CO₂ absorption process.
- (c) The intermolecular interaction intensity of several pure and mixed amines is analysed to assess solvent performance. The findings show that in comparison to pure 2EAE & 2DMAE and blended 2EAE/PZ, 2DMAE/PZ system, the blended system shows stronger intensity for all types of interactions.
- (d) The results pertaining to diffusivity shows that 2EAE exhibits the uppermost diffusivity while 2DMAE shows the lowest diffusivity than that of all selected amines. The order of diffusion rates within the amine system is as follows: EAE > MEA > DMAE > MAE-DEAB > MAE-DMA2P > EAE-TMPAD > AMP-PZ > EAE-DEAB > MAE-TMPAD > EAE-DMA2P > MAE-DMAE > EAE-DMAE > TMPAD > MEA-AMP > DMA2P > DMCA-MCA > DEAB > MEA-PZ. Higher diffusivity means the solvent should have faster reaction kinetics. The diffusivity results of 2EAE demonstrate that it can help to increase the reaction kinetics while combining with other amines.
- (e) Temperature exerts a substantial influence on the diffusivity of carbon dioxide (CO₂) within amines. When the temperature is elevated, the diffusivity of CO₂ within the amines experiences a pronounced increase i.e. it increases significantly at 333 K when compared to 313 K and 323 K. Particularly, the maximum diffusivity is seen for 2EAE at 333 K, showing temperature-dependent changes in diffusion behaviour. This increased diffusivity is a result of enhanced kinetic energy of the molecules, allowing for more efficient movement and interaction between molecules, which results in a more rapid mass transfer rate. The accelerated mass transfer rate has the potential to enable the design of smaller absorber units, which ultimately can lead to a reduction in energy consumption.

The study's practical implications are far-reaching and significant, since it proposes some unique solvent system (in pure and blended form) for CO₂ capture. The discovered solvent solution holds the prospect of dramatically improving carbon capture efficiency, potentially revolutionizing the approach to reducing greenhouse gas emissions. With lower energy consumption needs, this technology may help to minimize operational costs connected with carbon capture systems, making them more economically viable for widespread use across sectors. Therefore, additional investigations into the heat of absorption, kinetic properties of these mixtures and potential for regeneration is crucial for its practical applicability in carbon capture and industrial processes. Furthermore, a thorough exploration of the solvent's compatibility with various impurities commonly present in industrial gas streams (like SO_x and NO_x) is recommended to identify and address potential challenges.

CRedit authorship contribution statement

Maimoona Sharif: Writing – review & editing, Writing – original draft, Software, Methodology. **Tao Wang:** Writing – review & editing,

Supervision, Project administration, Funding acquisition. **Yanjie Xu:** Writing – review & editing. **Mengxiang Fang:** Supervision, Project administration. **Haiqian Wu:** Writing – review & editing. **Xiang Gao:** Writing – review & editing, Formal analysis.

Declaration of competing interest

The authors declare that they have no known competing financial interests or personal relationships that could have appeared to influence the work reported in this paper.

Data availability

the data is provided in a supplementary material file.

Acknowledgements

This study was supported by National Key R&D Program of China (2022YFB4101700), Pioneer R&D Program of Zhejiang Province (2023C03016) and the Fundamental Research Funds for the Central Universities (2022ZJFH04).

Appendix A. Supplementary data

Supplementary data to this article can be found online at <https://doi.org/10.1016/j.geoen.2024.212833>.

Abbreviations and Nomenclature

Symbol	Abbreviations
D(CO ₂)/m ² s ⁻¹	Diffusivity of CO ₂ /square meter per second
g(r)	Distance of atoms to interact with other atoms
m	Mass of particle
ns	Nanoseconds
ps	Picosecond
t	Time
r	Spherical radius
ρ	Density of atoms
r _i	Change in particle position
U	Potential energy
Å	Angstrom
E	Internal Energy
N	Number atoms
V	Volume
T	Temperature
wt%	Weight percentage
k	Boltzman's Constant
K	Kelvin
Ni	Atomic population

References

- Adeosun, A., Abu-Zahra, M.R., 2013. Evaluation of amine-blend solvent systems for CO₂ post-combustion capture applications. *Energy Proc.* 37, 211–218.
- Ahmad, M.Z., Hashim, H., Mustaffa, A.A., Maarof, H., Yunus, N.A., 2018. Design of energy efficient reactive solvents for post combustion CO₂ capture using computer aided approach. *J. Clean. Prod.* 176, 704–715.
- Anslyn, E.V., Dougherty, D.A., 2006. *Modern Physical Organic Chemistry*. University science books.
- Bavbek, O., Alper, E., 1999. Reaction mechanism and kinetics of aqueous solutions of primary and secondary alkanolamines and carbon dioxide. *Turk. J. Chem.* 23 (3), 293–300.
- San Diego, USA Biovia, *Material Studio*, 2020, 2017 Version 8.
- Bishnoi, S., Rochelle, G.T., 2000. Absorption of carbon dioxide into aqueous piperazine: reaction kinetics, mass transfer and solubility. *Chem. Eng. Sci.* 55 (22), 5531–5543.
- Caplow, M., 1968. Kinetics of carbamate formation and breakdown. *J. Am. Chem. Soc.* 90 (24), 6795–6803.
- Charati, S., Stern, S., 1998. Diffusion of gases in silicone polymers: molecular dynamics simulations. *Macromolecules* 31 (16), 5529–5535.
- ChemSpider, 2020. *ChemSpider Database*. Royal Society Of Chemistry [online]. 2020.

- Chen, D., Wang, Q., Li, Y., Li, Y., Zhou, H., Fan, Y., 2020. A general linear free energy relationship for predicting partition coefficients of neutral organic compounds. *Chemosphere* 247, 125869.
- Choi, W.-J., Seo, J.-B., Jang, S.-Y., Jung, J.-H., Oh, K.-J., 2009. Removal characteristics of CO₂ using aqueous MEA/AMP solutions in the absorption and regeneration process. *J. Environ. Sci.* 21 (7), 907–913.
- Ciftja, A.F., Hartono, A., Svendsen, H.F., 2013. Carbamate formation in aqueous-diamine-CO₂ systems. *Energy Proc.* 37, 1605–1612.
- Damartzis, T., Papadopoulos, A.I., Seferlis, P., 2016. Process flowsheet design optimization for various amine-based solvents in post-combustion CO₂ capture plants. *J. Clean. Prod.* 111, 204–216.
- Dey, A., Aroonwilas, A., 2009. CO₂ absorption into MEA-AMP blend: mass transfer and absorber height index. *Energy Proc.* 1 (1), 211–215.
- Donaldson, T.L., Nguyen, Y.N., 1980. Carbon dioxide reaction kinetics and transport in aqueous amine membranes. *Ind. Eng. Chem. Fund.* 19 (3), 260–266.
- Du, Y., Yuan, Y., Rochelle, G.T., 2016. Capacity and absorption rate of tertiary and hindered amines blended with piperazine for CO₂ capture. *Chem. Eng. Sci.* 155, 397–404.
- El Hadri, N., Quang, D.V., Goetheer, E.L., Zahra, M.R.A., 2017. Aqueous amine solution characterization for post-combustion CO₂ capture process. *Appl. Energy* 185, 1433–1449.
- EV, D., 2011. CO₂ Emissions from Fuel Combustion.
- Freeman, S.A., Rochelle, G.T., 2012. Thermal degradation of aqueous piperazine for CO₂ capture. 1. Effect of process conditions and comparison of thermal stability of CO₂ capture amines. *Ind. Eng. Chem. Res.* 51 (22), 7719–7725.
- Gao, Z., Ma, C., Lv, G., Li, A., Li, X., Liu, X., Yang, W., 2019. Car-Parrinello molecular dynamics study on the interaction between lignite and water molecules. *Fuel* 258, 116189.
- Gao, S., Zhang, Q., Su, X., Wu, X., Zhang, X.-G., Guo, Y., Li, Z., Wei, J., Wang, H., Zhang, S., 2023. Ingenious artificial leaf based on covalent organic framework Membranes for boosting CO₂ photoreduction. *J. Am. Chem. Soc.* 145 (17), 9520–9529.
- George, E.C., Riverol, C., 2020. Effectiveness of amine concentration and circulation rate in the CO₂ removal process. *Chem. Eng. Technol.* 43 (5), 942–949.
- Harun, N., Masiren, E., 2017a. Molecular dynamic simulation of amine-CO₂ absorption process. *Indian J. Sci. Technol.* 10 (2).
- Harun, N., Masiren, E.E., 2017b. Molecular dynamic simulation of CO₂ absorption into mixed aqueous solutions MDEA/PZ. *Chem. Eng. Res. Bull.* 19.
- Hill, T.L., 1986. An Introduction to Statistical Thermodynamics. Courier Corporation.
- Hunt, P.A., Ashworth, C.R., Matthews, R.P., 2015. Hydrogen bonding in ionic liquids. *Chem. Soc. Rev.* 44 (5), 1257–1288.
- Ibrahim, A., Ashour, F., Ghallab, A., Ali, M., 2014. Effects of piperazine on carbon dioxide removal from natural gas using aqueous methyl diethanol amine. *J. Nat. Gas Sci. Eng.* 21, 894–899.
- Idem, R., Edali, M., Aboudheir, A., 2009. Kinetics, modeling, and simulation of the experimental kinetics data of carbon dioxide absorption into mixed aqueous solutions of MDEA and PZ using laminar jet apparatus with a numerically solved absorption-rate/kinetic model. *Energy Proc.* 1 (1), 1343–1350.
- Idris, Z., Eimer, D.A., 2014. Representation of CO₂ absorption in sterically hindered amines. *Energy Proc.* 51, 247–252.
- Kadiwala, S., Rayer, A.V., Henni, A., 2012. Kinetics of carbon dioxide (CO₂) with ethylenediamine, 3-amino-1-propanol in methanol and ethanol, and with 1-dimethylamino-2-propanol and 3-dimethylamino-1-propanol in water using stopped-flow technique. *Chem. Eng. J.* 179, 262–271.
- Khan, A.A., Halder, G., Saha, A.K., 2019. Kinetic effect and absorption performance of piperazine activator into aqueous solutions of 2-amino-2-methyl-1-propanol through post-combustion CO₂ capture. *Kor. J. Chem. Eng.* 36, 1090–1101.
- Kim, D.Y., Lee, H.M., Min, S.K., Cho, Y., Hwang, I.-C., Han, K., Kim, J.Y., Kim, K.S., 2011. CO₂ capturing mechanism in aqueous ammonia: NH₃-driven Decomposition–recombination pathway. *J. Phys. Chem. Lett.* 2 (7), 689–694.
- Leach, A.R., 2001. *Molecular Modelling: Principles and Applications*. Pearson education.
- Liang, Y., Liu, H., Rongwong, W., Liang, Z., Idem, R., Solubility, P., Tontiwachwuthikul, 2015. Absorption heat and mass transfer studies of CO₂ absorption into aqueous solution of 1-dimethylamino-2-propanol. *Fuel* 144, 121–129.
- Liang, Z., Fu, K., Idem, R., Tontiwachwuthikul, P., 2016. Review on current advances, future challenges and consideration issues for post-combustion CO₂ capture using amine-based absorbents. *Chin. J. Chem. Eng.* 24 (2), 278–288.
- Lu, J., Wang, Sun, Li, J., 2005. Liu. Absorption of CO₂ into aqueous solutions of methyl diethanolamine and activated methyl diethanolamine from a gas mixture in a hollow fiber contactor. *Ind. Eng. Chem. Res.* 44 (24), 9230–9238.
- Masiren, E., Harun, N., Ibrahim, W., Adam, F., 2016a. Intermolecular interaction of monoethanolamine, diethanolamine, methyl diethanolamine, 2-Amino-2-methyl-1-propanol and piperazine amines in absorption process to capture CO₂ using molecular dynamic simulation approach. In: *The National Conference for Postgraduate Research 2016*.
- Masiren, E., Harun, N., Ibrahim, W., Adam, F., 2016b. Effect of temperature on diffusivity of monoethanolamine (MEA) on absorption process for CO₂ capture. *International Journal of Engineering Technology and Sciences* 3 (1), 43–51.
- Masiren, E.E., Harun, N., 2017. Comparison of different types of carbamate amine for stripping process. *Chemical Engineering Transactions* 56, 721–726.
- Masy, E., Vlugt, I.T., Pourquie, I.M., Besseling, I.N., Englebienne, P., Balaji, I.S., 2013. Predicting the Diffusivity of CO₂ in Substituted Amines. Delft University of Technology.
- Melnikov, S.M., Stein, M., 2019. The effect of CO₂ loading on alkanolamine absorbents in aqueous solutions. *Phys. Chem. Chem. Phys.* 21 (33), 18386–18392.
- Meunier, M., 2005. Diffusion coefficients of small gas molecules in amorphous cis-1, 4-polybutadiene estimated by molecular dynamics simulations. *The Journal of chemical physics* 123 (13), 134906.
- Miccio, F., Doghieri, F., Landi, E., 2015. Insights into high temperature sorbents for carbon dioxide. *Chemical Engineering Transactions* 43, 901–906.
- Muchan, P., Saiwan, C., Narku-Tetteh, J., Idem, R., Supap, T., Tontiwachwuthikul, P., 2017. Screening tests of aqueous alkanolamine solutions based on primary, secondary, and tertiary structure for blended aqueous amine solution selection in post combustion CO₂ capture. *Chem. Eng. Sci.* 170, 574–582.
- Mudhasakul, S., Ku, H.-m., Douglas, P.L., 2013. A simulation model of a CO₂ absorption process with methyldiethanolamine solvent and piperazine as an activator. *Int. J. Greenh. Gas Control* 15, 134–141.
- Naami, A., Edali, M., Sema, T., Idem, R., Tontiwachwuthikul, P., 2012. Mass transfer performance of CO₂ absorption into aqueous solutions of 4-diethylamino-2-butanol, monoethanolamine, and N-methyldiethanolamine. *Ind. Eng. Chem. Res.* 51 (18), 6470–6479.
- Neveux, T., Le Moullec, Y., Corriou, J.P., Favre, E., 2013. Energy performance of CO₂ capture processes: interaction between process design and solvent. *Chem Eng Trans* 35, 337–342.
- Papadopoulos, A.I., Seferlis, P., 2017. *Process Systems and Materials for CO₂ Capture*. Wiley Online Library.
- Raksajati, A., Ho, M., Wiley, D., 2018. Solvent development for post-combustion CO₂ Capture: Recent development and opportunities. In: *MATEC Web of Conferences*. EDP Sciences.
- Rangwala, H., Morrell, B., Mather, A., Otto, F., 1992. Absorption of CO₂ into aqueous tertiary amine/MEA solutions. *Can. J. Chem. Eng.* 70 (3), 482–490.
- Sartori, G., Savage, D., 1983. Sterically hindered amines for carbon dioxide removal from gases. *Ind. Eng. Chem. Fundam.* 22 (2), 239–249.
- Sema, T., 2012. Kinetics of Carbon Dioxide Absorption into Aqueous Solutions of 4-(diethylamino)-2-Butanol and Blended Monoethanolamine and 4-(diethylamino)-2-Butanol. The University of Regina (Canada).
- Sema, T., Naami, A., Idem, R., Tontiwachwuthikul, P., 2011. Correlations for equilibrium solubility of carbon dioxide in aqueous 4-(diethylamino)-2-butanol solutions. *Ind. Eng. Chem. Res.* 50 (24), 14008–14015.
- Sharif, M., Zhang, T., Wu, X., Yu, Y., Zhang, Z., 2020. Evaluation of CO₂ absorption performance by molecular dynamic simulation for mixed secondary and tertiary amines. *Int. J. Greenh. Gas Control* 97, 103059.
- Sharif, M., Wu, X., Yu, Y., Zhang, T., Zhang, Z., 2022. Estimation of diffusivity and intermolecular interaction strength of secondary and tertiary amine for CO₂ absorption process by molecular dynamic simulation. *Mol. Simulat.* 48 (6), 484–494.
- Sharif, M., Fan, H., Sultan, S., Yu, Y., Zhang, T., Wu, X., Zhang, Z., 2023a. Evaluation of CO₂ absorption and stripping process for primary and secondary amines. *Mol. Simulat.* 49 (6), 565–575.
- Sharif, M., Fan, H., Wu, X., Yu, Y., Zhang, T., Zhang, Z., 2023b. Assessment of novel solvent system for CO₂ capture applications. *Fuel* 337, 127218.
- Sharif, M., Han, T., Wang, T., Shi, X., Fang, M., Shuming, D., Meng, R., Gao, X., 2024. Investigation of rational Design of amine Solvents for CO₂ capture: a computational approach. *Chem. Eng. Res. Des.* 204, 524–535.
- Singto, S., Supap, T., Idem, R., Tontiwachwuthikul, P., Tantayanon, S., Al-Marri, M.J., Benamor, A., 2016. Synthesis of new amines for enhanced carbon dioxide (CO₂) capture performance: The effect of chemical structure on equilibrium solubility, cyclic capacity, kinetics of absorption and regeneration, and heats of absorption and regeneration. *Separ. Purif. Technol.* 167, 97–107.
- Sodiq, A., Hadri, N.E., Goetheer, E.L., Abu-Zahra, M.R., 2018. Chemical reaction kinetics measurements for single and blended amines for CO₂ postcombustion capture applications. *Int. J. Chem. Kinet.* 50 (9), 615–632.
- Tan, Y.H., 2010. Study of CO₂-absorption into Thermomorphic Lipophilic Amine Solvents.
- Vaidya, P.D., Kenig, E.Y., 2007. CO₂-alkanolamine reaction kinetics: a review of recent studies. *Chem. Eng. Technol.: Industrial Chemistry-Plant Equipment-Process Engineering-Biotechnology* 30 (11), 1467–1474.
- Van Wagener, D.H., Rochelle, G.T., 2011. Stripper configurations for CO₂ capture by aqueous monoethanolamine and piperazine. *Energy Proc.* 4, 1323–1330.
- Vega, F., Cano, M., Camino, S., Navarrete, B., Camino, J., 2018. Evaluation of the absorption performance of amine-based solvents for CO₂ capture based on partial oxy-combustion approach. *Int. J. Greenh. Gas Control* 73, 95–103.
- Wang, L., Liu, S., Wang, R., Li, Q., Zhang, S., 2019. DMCA-MCA hybrid with high absorption rate and low energy penalty for CO₂ capture. In: *International Conference on Applied Energy*, 2019.
- Wang, R., Liu, S., Li, Q., Zhang, S., Wang, L., An, S., 2021. CO₂ capture performance and mechanism of blended amine solvents regulated by N-methylcyclohexylamine. *Energy* 215, 119209.
- Wang, Z., Fernández-Blanco, C., Chen, J., Veiga, M.C., Kennes, C., 2024. Effect of electron acceptors on product selectivity and carbon flux in carbon chain elongation with Megasphaera hexanoica. *Sci. Total Environ.* 912, 169509.
- Xiao, J., Li, C.-W., Li, M.-H., 2000. Kinetics of absorption of carbon dioxide into aqueous solutions of 2-amino-2-methyl-1-propanol+ monoethanolamine. *Chem. Eng. Sci.* 55 (1), 161–175.
- Yao, X., Yu, X., Wang, L., Zeng, Y., Mao, L., Liu, S., Xie, H., He, G., Huang, Z., Liu, Z., 2023. Preparation of cinnamic hydroxamic acid collector and study on flotation characteristics and mechanism of scheelite. *Int. J. Min. Sci. Technol.* 33 (6), 773–781.
- Ye, Q., Wang, X., Lu, Y., 2015. Screening and evaluation of novel biphasic solvents for energy-efficient post-combustion CO₂ capture. *Int. J. Greenh. Gas Control* 39, 205–214.

- Zeebe, R.E., 2011. On the molecular diffusion coefficients of dissolved CO₂, HCO₃⁻, and CO₃²⁻ and their dependence on isotopic mass. *Geochem. Cosmochim. Acta* 75 (9), 2483–2498.
- Zhang, X., 2007. Studies on multiphase CO₂ capture systems. *Fortschr.-Ber. VDI, Reihe 3 Verfahrenstechnik* 884.
- Zhang, J., 2014. Study on CO₂ Capture Using Thermomorphic Biphasic Solvents with Energy Efficient Regeneration. *Universitätsbibliothek Dortmund*.
- Zhang, J., Agar, D.W., Zhang, X., Geuzebroek, F., 2011. CO₂ absorption in biphasic solvents with enhanced low temperature solvent regeneration. *Energy Proc.* 4, 67–74.
- Zhang, J., Qiao, Y., Wang, W., Misch, R., Hussain, K., Agar, D.W., 2013. Development of an energy-efficient CO₂ capture process using thermomorphic biphasic solvents. *Energy Proc.* 37, 1254–1261.
- Zhang, R., Liang, Z., Liu, H., Rongwong, W., Luo, X., Idem, R., Yang, Q., 2016. Study of formation of bicarbonate ions in CO₂-loaded aqueous single 1DMA2P and MDEA tertiary amines and blended MEA–1DMA2P and MEA–MDEA amines for low heat of regeneration. *Ind. Eng. Chem. Res.* 55 (12), 3710–3717.
- Zhang, S., Shen, Y., Shao, P., Chen, J., Wang, L., 2018. Kinetics, thermodynamics, and mechanism of a novel biphasic solvent for CO₂ capture from flue gas. *Environ. Sci. Technol.* 52 (6), 3660–3668.
- Zhang, S., Bai, X., Zhao, C., Tan, Q., Luo, G., Wang, J., Xi, H., 2021. Global CO₂ consumption by silicate rock chemical weathering: its past and future. *Earth's Future* 9 (5), e1938E–e2020E.
- Zhang, Q., Gao, S., Guo, Y., Wang, H., Wei, J., Su, X., Zhang, H., Liu, Z., Wang, J., 2023. Designing covalent organic frameworks with Co-O4 atomic sites for efficient CO₂ photoreduction. *Nat. Commun.* 14 (1), 1147.
- Zhao, R., Huang, X., Xue, J., Guan, X., 2023. A practical simulation of carbon sink calculation for urban buildings: a case study of Zhengzhou in China. *Sustain. Cities Soc.* 99, 104980.
- Zhao, X., Fan, B., Qiao, N., Soomro, R.A., Zhang, R., Xu, B., 2024. Stabilized Ti3C2Tx-doped 3D vesicle polypyrrole coating for efficient protection toward copper in artificial seawater. *Appl. Surf. Sci.* 642, 158639.
- Zhou, X., Liu, F., Lv, B., Zhou, Z., Jing, G., 2017. Evaluation of the novel biphasic solvents for CO₂ capture: performance and mechanism. *Int. J. Greenh. Gas Control* 60, 120–128.